Lattice relaxation and electric field gradients in impurity-doped single ionic crystals

Mitsuo Satoh and Toshihiko Taki
Faculty of Engineering, Tokushima University, Tokushima 770, Japan
and Technical College, Tokushima University, Tokushima 770, Japan
(Received 6 June 1980)

The lattice relaxation parameters in several ionic crystals doped with monovalent impurity ions are calculated by energy minimization taking account of the Coulomb, overlap-repulsive and three-body potential energies, the last of which was developed early in calculation of the cohesive energy of ionic crystals by Löwdin. The displaced 256 ions around one substitutional impurity ion are taken into consideration and the results are utilized to calculate the electric field gradient (EFG) at the similar sites to (1,0,0), (1,1,0), (1,1,1), (2,0,0), and (2,1,0) sites relative to the impurity at (0,0,0). Both experimental and theoretical EFG's, types and asymmetry parameters of the EFG tensors are compared with each other by using Löwdin-Satoh-Taki or Ra-Abarenkov-Antonova models. The theoretical values of the crystals which do not contain the potassium ions as the impurity or as the host ions, in both models, agree fairly well with the experimental ones if we consider only nearest-neighbor overlaps. With respect to the crystals containing these ions, agreement is also satisfactory when we assume a small quantity of covalency (several percent) between the nearest-neighbor cation and anion, where the extraordinarily large overlaps exist. On the other hand, the results of this study by using both models show that the overlap integrals between the second-neighbor anion and anion in the practical crystals will be extremely small compared with large values of those integrals obtained from the atomic orbitals of the free ions.

I. INTRODUCTION

In the preceding paper,[1] referred to as RII hereafter, we obtained the experimental values of the quadrupole frequency ν_Q, the electric field gradient (EFG), eq and the asymmetry parameter η of the EFG at various sites around the monovalent substitutional impurity ion in the impurity-doped single ionic crystals. It was a most remarkable fact that the measured η's at (1,1,0) sites are fairly small values and nearly equal for NaCl-Br, NaBr-Cl, NaCl-I, NaBr-I, and NaCl-K crystals which are inconsistent with the previous theory on the EFG[2–5] giving the different eq's and very large η's. Another lattice-relaxation (the displacements of ions due to impurity substitution) approach in a number of alkali halides containing monovalent impurity ions was performed and gave a good agreement with the calorimetric data of heats.[6] However, our calculation of the EFG[7,8] by using both lattice-relaxation parameters and the electronic polarization of the ions obtained from this approach also gives disagreement with the empirical data, and it is nearly independent of choice of the polarizabilities of the ions.

In calculation of both approaches the Born-Mayer (BM) model of ionic crystals was adopted and the Coulomb and the overlap-repulsive energies were considered. This model succeeds quite well concerning calculations of the cohesive energy using observed lattice constants and bulk moduli. It is unsuccessful in computing the elastic shear modulus and the dielectric constants of these crystals. The EFG at (1,1,0) sites around impurity ions seems to be related to the problem of the shear modulus. On the other hand, the overlap distortions of the electron wave functions around the impurities were investigated and their influences on the EFG were obtained by Ikenberry and Das.[9] The experimental eq at Na (1,0,0) sites in NaCl-Br in RII agrees with their calculation. However, their computations for the other crystals do not agree with the empirical data, for instance, the eq at Cl(1,0,0) in NaCl-K obtained from Slusher and Hahn's and our experimental data, and also that of Br(1,0,0) in KBr-Na obtained from Andersson's experiments are very different from Ikenberry and Das's calculated values.

Löwdin derived quantum mechanically the cohesive energy, the interionic distance and elastic constants of some ionic crystals by using the Hartree-Fock wave functions of the free ions and obtained very good agreement with the empirical data.[10,11] The two-body term among the many-body potentials will be contained within the overlap repulsion in the BM semiempirical theory. The three-body term has an important role for Löwdin's theoretical values of the pure ionic crystals and is not included

 ©1981 The American Physical Society

in the BM model, whereas the higher terms than this potential give only a small contribution. It was expected that in this study of the ionic crystals doped with impurity ions, the three-body potential should play an important part in the lattice relaxation. A modified form of the three-center integrals was developed by Löwdin.[11] This form produces the two-point-charge model effectively, instead of the actual overlap-charge distribution. This model applied by us for the impurity-doped crystals will be denoted as Löwdin-Satoh-Taki (LST) model hereafter.

Another approximation was adopted by Ra,[12] Abarenkov, and Antonova.[13] In Ra's paper the cohesive energies and short-range force constants in alkaline-earth fluorides were calculated with three-body interactions, and in the latter two-body and three-body potentials in several alkali halides were computed. From this approximation the three-point-charge model is derived which will be called Ra-Abarenkov-Antonova (RAA) model hereafter. Their calculations were carried out for the pure or homogeneously deformed crystals and it was recognized that three-body terms between the second-neighbor anion and anion are as important as those of the nearest-neighbor cation-anion pair, in both studies.

In order to calculate the change of the three-body potentials due to impurity substitution, these approximations are essential and very effective means of facilitating the calculations. If the actual overlap-charge distributions are used to compute this potential change, the tremendously many programs are necessary for computer calculations and it will take effort to make them.

The overlap integrals of the nearest neighbors and those of the next-nearest-neighbor ions in pure ionic crystals have been calculated by many investigators.[10,11,14,15] In the present study with the impurities one needs the overlap integrals of the host ion pair and also those of the impurity-host ion pair in the crystals. Therefore we have computed many integrals and their dependence on the lattice distance by using the α-function technique,[10,11] as shown in our preceding paper,[16] referred to as RI hereafter.

Townes and Dailey have shown early that existence of the covalent bonding causes a large EFG at the position of the nucleus.[17] The covalency in H_2, F_2, or HF molecules was studied in connection with the chemical shifts σ of the nuclear magnetic resonance (NMR) lines.[18,19] Then the effects of covalency on the chemical shifts and the spin-lattice relaxation time T_1 of the NMR in pure ionic crystals were investigated and the degree of covalency in some ionic crystals was estimated from the observed chemical shifts.[20,21] Afterwards, however, it was reported that the overlaps between the electron orbitals in the nearest-neighbor ions also affect the σ and T_1 in ionic crystals.[22]

In the present study both overlap and covalency affect the lattice relaxation and their effects can be computed separately. We have calculated the lattice-relaxation parameters in the alkali halides with the impurities by using LST or RAA model and obtained the EFG and the η values at the near sites around the impurity ions from these parameters. The new characteristics of the present study are as follows.

(a) Inclusion of the three-body potentials within the potential energies.

(b) Consideration of the electron-shell deformations due to the displacements of the concerned ions. Both are very important for calculations of the EFG since the previous computations[2–5] of the EFG without them cannot explain most of the experimental results.

(c) Adoption of three adjustable parameters for calculation of the EFG. The Sternheimer antishielding factors and the proportionality constants connected with (b) above have been used as the parameters to adjust the calculated EFG's to the empirical ones. However, these parameters are not chosen for every crystal, but each one for each approximation above mentioned, is adopted. For the crystals containing K^+ ions, covalencies have been also used as the third parameters.

(d) Classification of the types of the EFG tensors at the (1,1,0) sites in the crystals. The EFG-tensor types at the (1,1,0) sites have been classified by us. The types *A* and *D* in this classification were found by the other investigators theoretically and experimentally.[4,5,30–34] However, types *B* and *C* have been found by us in both ways, in the RII[1] and this study for the first time. The calculated values of the EFG's, η's and these types at these sites have been compared with those obtained from the experiments and generally good agreements have been obtained, though one needs the parameters as described in (c).

(e) Taking the many movable ions around impurities into consideration. While the previous investigators took only 26,[2,3] 56,[4,5,9] or 96[6] movable ions, we have taken 256 ions around one impurity ion into consideration. This enables us to calculate the lattice-relaxation parameters and the EFG's more accurately, though the calculations will be complicated.

In Sec. II the changes in Coulomb, overlap-repulsive and three-body potentials due to impurity substitution are described. The constants used in this study and the overlap pairs are represented in the next section. The calculations of the three-body potentials by using two different (LST and RAA) models are given in Secs. IV and V. In Sec. VI the computations of EFG's are described and the types of the EFG tensors at the (1,1,0) sites are classified. The results of calculations on the lattice-relaxation parameters and EFG's by using the methods described in above sections are compared with the experimental data in A and B of Sec. VII. In C and

D of this section influence of covalent bondings on the EFG, and calculation including both nearest- and next-nearest-neighbor overlap integrals are described, respectively. Summary and conclusions are given in the last section.

II. ENERGY CHANGE AFTER IMPURITY SUBSTITUTION

As mentioned in the Introduction, the change of the total potential energy after substitution of the monovalent impurity ions in ionic crystals will be

$$\Delta E = \Delta E_C + \Delta E_R + \Delta E_T \ , \tag{1}$$

where the first term in the right-hand side expresses the change in the total Coulomb energy among the ions which have, as usual, the point charges $+e$ or $-e$ ($-e$ is an electronic charge), the second, that of the repulsive energy arising from the overlaps between electron orbitals of the nearest-neighbor ions, and those between the next-nearest-neighbor ions and the third, that of the three-center integrals which is related to three nuclei as shown in Fig. 1 as an example.[10] Although we can understand this term also as a change of the Coulomb energy, it will be conveniently distinguished from ΔE_C as the BM theory does not include this term. As described in the next, we have adopted the BM theory for the second term, ΔE_R and this theory contains the two-body terms. Therefore, the two-body terms should be strictly excluded from calculations of ΔE_T in the computer programs though exclusion of them is the complicated work. Normalization of the electron charge produces the change of the ionic charge, above-mentioned $\pm e$ if there are overlap charges. However, we will follow Löwdin's method[10,11] and treat this change together with the overlap charges as shown in the three-body potentials of Eq. (4). This method is convenient for computer calculations.

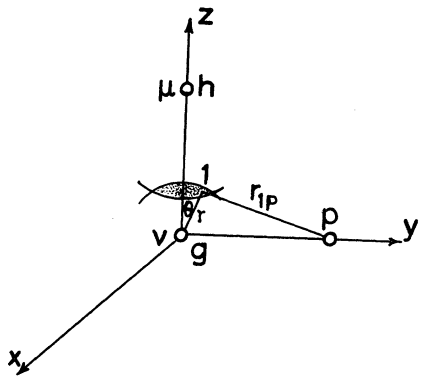

FIG. 1. The three-center integral which is a potential energy of the overlapping charge between g and h ions, due to the third ion p, as an example. In this study μ and ν represent the atomic orbitals in the anion h and cation g, respectively.

The changes in the Coulomb energy are calculated by using a method of the dipole-dipole interactions and the terms up to the J ions (designation of the displaced ions is given in Table I of the next section) are in good agreement with the values available from Douglas's paper.[6] For the overlap-repulsive energy, Huggins-Mayer-type potentials are used including both the overlaps between the nearest-neighbor ions and those between the next-nearest-neighbor ions.

If symmetric orthogonalization is applied for atomic orbitals (AO's) of the ions, the three-body potential in atomic units is represented as follows[10,11]:

$$E_T = \tfrac{1}{2} {\sum_{g,h}}' T(g,h) \ , \tag{2}$$

$$T(g,h) = \sum_{p \neq g,h} t(g,h,p) \ , \tag{3}$$

$$t(g,h,p) = 2\epsilon_p \sum_{\mu}^{(h)} \sum_{\nu}^{(g)} \left[2S_{\mu\nu} \int \frac{\Phi_\mu^*(1)\Phi_\nu(1)}{r_{1p}} dv_1 - S_{\mu\nu}^2 \left\{ \int \frac{\Phi_\mu^*(1)\Phi_\mu(1)}{r_{1p}} dv_1 + \int \frac{\Phi_\nu^*(1)\Phi_\nu(1)}{r_{1p}} dv_1 \right\} \right] \ , \tag{4}$$

where ϵ_p, r_{1p}, $S_{\mu\nu}$ are the charge of the ion p, the distance between referred electron 1 and p ion, and the overlap integral between μ and ν electron orbitals. The Φ_μ and Φ_ν express one-electron orbitals of the free ion; $\sum_\mu^{(h)}$, the sum over all orbitals of ion h; $\frac{1}{2}{\sum_{g,h}}'$, the sum over all different pairs of ions. Although procedure of symmetric orthogonalization is not necessarily correct for the crystals with the local lattice deformation, yet it seems important to study the effect of the three-body potentials with this procedure before a perfect theory will become available. Expanding $1/r_{1p}$ in the second term of Eq. (4) into spherical harmonics about the ion h, we have the next approximation[13]

$$-\sum_{\mu}^{(h)} \sum_{\nu}^{(g)} S_{\mu\nu}^2 \int \frac{\Phi_\mu^*(1)\Phi_\mu(1)}{r_{1p}} dv_1 \simeq -\frac{M_0(g,h)}{r_{hp}} - \frac{M_h(g,h)(3\cos^2\theta_{ghp} - 1)}{r_{hp}^3} \ , \tag{5}$$

TABLE I. Identification of ion shells and Cartesian coordinates of their ions in units of R_0 after impurity substitution.

Shell No.	Name of shell	No. of ions	Coordinates
0	O	1	0,0,0
1	A	6	$1+a$,0,0
2	B	12	$1+b, 1+b$,0
3	C	8	$1+c, 1+c, 1+c$
4	D	6	$2+2d$,0,0
5	E	24	$2+2e, 1+f$,0
6	G	24	$2+2g, 1+h, 1+h$
7	I	12	$2+2i, 2+2i$,0
8	J	6	$3+j$,0,0
9	K	24	$2+2k, 2+2k, 1+l$
10	M	24	$3+3m, 1+n$,0
11	P	24	$3+3p, 1+p, 1+p$
12	Q	8	$2+2q, 2+2q, 2+2q$
13	R	24	$3+3r, 2+2s$,0
14	T	48	$3+3t, 2+2t, 1+t$
15	U	6	$4+4u$,0,0
16			3,2,2
17			4,1,0
18			3,3,0
19			4,1,1
20			3,3,1
21			4,2,0
22			4,2,1
23			5,0,0

where θ_{ghp} is the angle between vectors $\vec{r}_g - \vec{r}_h$ and $\vec{r}_p - \vec{r}_h$, and

$$M_0(g,h) = \sum_{\mu}^{(h)} \sum_{\nu}^{(g)} S^2_{\mu\nu} \ , \tag{6}$$

$$M_h(g,h) = \tfrac{1}{5} \sum_{\nu}^{(g)} (S^2_{n\mu p\mu 0,\nu} - S^2_{n\mu p\mu 1,\nu}) \int_0^\infty P^2_{n\mu p\mu}(r) r^2 dr, \quad \mu \in h \ , \tag{7}$$

where $P_{n\mu p\mu}$ is the normalized radial wave function. The third term in Eq. (4) is approximated in the same way as the second one. For treating the first term in Eq. (4), two different ways have appeared so far. One of them was shown by Löwdin[11] for the pure ionic crystals and was applied by us for the impurity-doped crystals. It is the LST model as mentioned in the Introduction. Another one was adopted by Ra[12] and by Abarenkov and Antonova[13] (RAA model). These two models calculating the three-body potential will be stated separately in Secs. IV and V.

Before the detailed description of both models, the constants and variables taken in this study will be explained in the next section.

III. CHOICE OF CONSTANTS AND VARIABLES, OVERLAP PAIRS AND CHANGE OF PAIR DISTANCE

As shown in Table I, the displaced 256 ions classified into 15 groups with displacements $a, \ldots, u$ in units of R_0 around one substitutional impurity ion in the crystals are taken into consideration, where R_0 is the nearest-neighbor distance in perfect salts in cgs units, and further 8 groups of the undisplaced ions are included in calculations in order to complete the overlapping pair of the displaced ions. The reason why so many displaced ions should be taken is to calculate the EFG at various sites as accurately as possible, by means of including the effects of the distant

TABLE II. Overlap pairs and the change of pair distance, ϵ in units of R_0.

Overlap pair	No. of overlap pairs	Change of pair distance, ϵ
O-A	6	a
A-D	6	$2d-a$
D-J	6	$3j-2d$
A-B	24	$b+\frac{1}{2}a^2+\frac{1}{2}b^2-ab$
B-C	24	$c+b^2+c^2-2bc$
B-E	24	$-b+2e+\frac{1}{2}(b^2+f^2)-bf$
D-E	24	$f+2(d^2+e^2)-4de$
C-G	24	$-c+2g+c^2+h^2-2ch$
E-G	48	$h+2(e^2+g^2)+\frac{1}{2}(f^2+h^2)-4eg-fh$
E-I	24	$-f+2i+2(e^2+i^2)-4ei$
E-M	24	$3m-2e+\frac{1}{2}(f^2+n^2)-nf$
J-M	24	$n+(\frac{9}{2})(j^2+m^2)-9jm$
G-K	48	$2k-h+2(g^2+k^2)+\frac{1}{2}(h^2+l^2)-4gk-hl$
I-K	24	$l+4(i^2+k^2)-8ik$
G-P	24	$3p-2g+h^2+p^2-2hp$
I-R	24	$3r-2i+2(i^2+s^2)-4is$
J-U	6	$4u-3j$
K-Q	24	$2q-l+4(k^2+q^2)-8kq$
K-T	48	$3t-2k+2(k^2+t^2)-4kt+\frac{1}{2}(l^2+t^2)-lt$
M-P	48	$p+(\frac{9}{2})m^2+\frac{1}{2}n^2+5p^2-9mp-np$
M-R	24	$2s-n+(\frac{9}{2})(m^2+r^2)-9mr$
M-17	24	$-3m+\frac{1}{2}n^2$
P-T	48	$2t-p+5(p^2+t^2)-10pt$
P-19	24	$-3p+p^2$
Q-16	24	$-2q+4q^2$
R-T	48	$t+(\frac{9}{2})r^2+2s^2+(\frac{13}{2})t^2-9rt-4st$
R-18	24	$-2s+(\frac{9}{2})r^2$
R-21	24	$-3r+2s^2$
T-16	48	$-t+(\frac{13}{2})t^2$
T-20	48	$-2t+5t^2$
T-22	48	$-3t+(\frac{5}{2})t^2$
U-17	24	$8u^2$
U-23	6	$-4u$

displaced ions from the impurity ions.

For R_0, the same values have been used as those of Douglas[6] which are somewhat smaller than the usual. However, these distances will be suitable for our study since our data have been obtained at low temperature as described in RII. We have adopted the Tessman, Kahn, and Shockley's (TKS) values for the polarizabilities α of the ions throughout this study.[23] Other polarizabilities[4] also have been tried and the various quantities in the EFG are nearly independent of the polarizabilities, calculations of which will be included in Sec. VII B.

The nearest-neighboring ion pair whose electron orbitals overlap each other, and the change of the pair distance ϵ after impurity substitution, are calculated by using the displacements $a, \ldots, u$ of the pair ions as shown in Table II. The similar table concerned with the second-neighbor ions is also obtained

in the same way. These tables are utilized in the calculation of dependence of the overlap integrals on the lattice deformation in Secs. IV and V.

IV. LST MODEL

For practical applications of Eq. (4), a modified form was developed by Löwdin.[11] Expanding the given Hartree-Fock AO's Φ_ν and Φ_μ in terms of the complete systems $(\Phi_{\mu'})$ and $(\Phi_{\nu'})$ constructed around the nuclei g_μ and g_ν, respectively, we obtain

$$\Phi_\nu = \sum_{\mu'} \Phi_{\mu'} S_{\mu'\nu}, \quad \Phi_\mu = \sum_{\nu'} \Phi_{\nu'} S_{\nu'\mu} \ . \tag{8}$$

Introducing two arbitrary multipliers λ_1 and λ_2 satisfying the condition $\lambda_1 + \lambda_2 = 1$, we have for the real density

$$\Phi_\mu \Phi_\nu = \lambda_1 \sum_{\mu'} \Phi_\mu \Phi_{\mu'} S_{\mu'\nu} + \lambda_2 \sum_{\nu'} \Phi_{\nu'} \Phi_\nu S_{\nu'\mu} \ . \tag{9}$$

If μ' and ν' are summed over all orbitals $\bar{\mu}$ and $\bar{\nu}$ belonging to the same and lower principal quantum numbers than μ and ν, respectively, this form of the charge density gives a very good approximation to the nuclear attraction integrals. The right hand of Eq. (9) has the correct total charge $\int \Phi_\mu \Phi_\nu \, dv_1 = S_{\mu\nu}$ and the best values of the multipliers λ_1 and λ_2 may be chosen so that the total electric dipole moment μ_z along the line μ-ν would be given correctly. The calculated values of μ_z and their dependence on the nearest-neighbor distance in some alkali halides have been already obtained utilizing two-center integrals I_i as shown in RI.

First we shall investigate the case of outer-shell electrons, then we have following five kinds of $S_{\mu\nu}$ between the overlapping orbitals μ and ν. For (i), $\Phi_\nu = ns$, the orbital of a cation and $\Phi_\mu = n's$, that of an anion where both orbitals overlap each other, we get from the RI using Eq. (9),

$$\begin{aligned} I_1 - \tfrac{1}{2} a S_{n's;ns} = {} & \lambda_1^{(1)} S_{n'p0;ns} \int \Phi_{n's} \Phi_{n'p0} r \cos\theta \, dv_1 \\ & + \lambda_2^{(1)} S_{np0;n's} \int \Phi_{ns} \Phi_{np0} r \cos\theta \, dv_1 \\ & + \tfrac{1}{2} a S_{n's;ns} (\lambda_1^{(1)} - \lambda_2^{(1)}) \ , \end{aligned} \tag{10}$$

where r, θ, and ϕ represent the spherical coordinates of the electron 1, and "a" is the nearest-neighbor distance in atomic units and both μ- and ν-quantized axes were chosen as the positive z axis in Fig. 1 in the same way as that used by Hafemeister and Flygare.[15] When Φ_μ and Φ_ν are the AO's of anion and cation respectively, for (ii), $\Phi_\nu = np0$, $\Phi_\mu = n's$, (iii), $\Phi_\nu = ns$, $\Phi_\mu = n'p0$, (iv), $\Phi_\nu = np0$, $\Phi_\mu = n'p0$, we have obtained three equations similar to Eq. (10). For (v), $\Phi_\nu = np1$, $\Phi_\mu = n'p1$, we have a simple equation:

$$I_5 - \tfrac{1}{2} a S_{n'p1;np1} = \tfrac{1}{2} a S_{n'p1;np1} (\lambda_1^{(5)} - \lambda_2^{(5)}) \ , \tag{11}$$

because of vanishing of $S_{n's;np1}$ and $S_{ns;n'p1}$.

Löwdin took the μ- and ν-quantized axes to directions of negative and positive z axes, respectively, therefore in the methods of Löwdin and Hafemeister-Flygare, the signs of the overlap integrals containing the anion $p0$ orbitals, $S_{n'p0;ns}$ and $S_{n'p0;np0}$ are different from each other. If we use Löwdin's quantized axes, then a negative sign should be added to the first term of the right hand in Eq. (10), and so on in (ii), (iii), and (iv) cases, accordingly we have the same $\lambda_1^{(i)}$ and $\lambda_2^{(i)}$ values $(i = 1, \ldots, 5)$, respectively, in both methods. For the practical use of Eq. (10), consequently, it will be convenient to take the absolute values of I and S in Eq. (10) and in the similar equations. Then we obtain the same equations for both methods as follows:

$$\begin{aligned} |I_1| - \tfrac{1}{2} a |S_1| = {} & -\lambda_1^{(1)} |S_3| \int \Phi_{n's} \Phi_{n'p0} r \cos\theta \, dv_1 \\ & - \lambda_2^{(1)} |S_2| \int \Phi_{ns} \Phi_{np0} r \cos\theta \, dv_1 \\ & + \tfrac{1}{2} a |S_1| (\lambda_1^{(1)} - \lambda_2^{(1)}) \ , \end{aligned} \tag{12}$$

and three similar equations, where abbreviations $S_1 = S(n's|ns)$, $S_2 = S(n's|np0)$, $S_3 = S(n'p0|ns)$, and $S_4 = S(n'p0|np0)$ were used for convenience in the same fashion as I_i in RI. Since the integrals of the first and second terms in the right-hand side of Eq. (12) are single-center integrals, they are easily calculated as shown in Table II of RI and are independent upon the change of the nearest-neighbor distance distinctly from all other quantities of this equation. For Eq. (11), we have

$$|I_5| - \tfrac{1}{2} a |S_5| = \tfrac{1}{2} a |S_5| (\lambda_1^{(5)} - \lambda_2^{(5)}) \ , \tag{13}$$

with an abbreviation $S_5 = S(n'p1|np1)$.

So far only the outer-shell electrons have been treated. Here we will consider the inner-shell electrons simultaneously. Most overlap integrals containing inner-shell electrons are very small and negligible compared with those between outer-shell electrons. However, the $1s$ in Na^+ ions and $2s$, $2p$ electrons in K^+ ions have some contribution in our studies. When we take the inner-shell electrons, two contributions to the overlapping charges are generally considered. First, the overlap between the inner-shell electron and outer one contributes directly to the overlap charges as shown in Table V of the RI, which also produces $\lambda_1^{(i)}$ and $\lambda_2^{(i)}$ $(i = 6, 7, \ldots,)$ in ways similar to Eq. (12). Secondly, these overlap integrals accompanied by such single-center integrals as shown on the last five rows in Table II of RI are added to the second term of the right-hand side in Eq. (12) and modify the $\lambda_1^{(i)}$ and $\lambda_2^{(i)}$ values $(i = 1, \ldots, 4)$

slightly.

We expand the next quantities with respect to ϵ. These expansions are possible when $R_0\epsilon \ll \rho$ or σ (see Table II in this text and Tables III, IV, and V in RI) as is the case in this study. Then we have

$$\lambda_1^{(i)} = \lambda_X^{(i)} + \lambda_Y^{(i)}\epsilon + \lambda_Z^{(i)}\epsilon^2, \quad \lambda_2^{(i)} = 1 - \lambda_1^{(i)} \ , \tag{14}$$

$$|I_i| = X_{Ii} + Y_{Ii}\epsilon + Z_{Ii}\epsilon^2 \ , \tag{15}$$

$$|S_i| = X_{Si} + Y_{Si}\epsilon + Z_{Si}\epsilon^2 \quad (i=1,\ldots,4) \ , \tag{16}$$

$$-a = \gamma + \gamma\epsilon = -a_0(1+\epsilon) \ , \tag{17}$$

where a_0 represents the nearest-neighbor distance in the perfect crystal in a.u. For the outer-shell electrons in the anion,

$$\alpha = -\int \Phi_{n's}\Phi_{n'p0} r\cos\theta d\upsilon_1 \ , \tag{18}$$

and for the outer-shell electrons in the cation,

$$\beta = -\int \Phi_{ns}\Phi_{np0} r\cos\theta d\upsilon_1 \ . \tag{19}$$

On the other hand,

$$\beta' = \int \Phi_{An''s}\Phi_{Anp0} r\cos\theta d\upsilon_1 \ , \tag{20}$$

where $A=$Na, $n''=1$, $n=2$ for $i=2, 4$ of the Na ion, while, $A=$K, $n''=3$, $n=2$ for $i=1, 3$ of the K ion, and $A=$K, $n''=2$, $n=3$ for $i=2, 4$ of the K ion, respectively. And also we have

$$|S_j'| = X_{Sj}' + Y_{Sj}'\epsilon + Z_{Sj}'\epsilon^2 \ , \tag{21}$$

where $j=1$ for $S(\mathrm{Na}1s|n's)$ and $j=3$ for $S(\mathrm{Na}1s|n'p0)$ or $j=1,2,3$, and 4 for $S(\mathrm{K}2s|n's)$, $S(\mathrm{K}2p0|n's)$, $S(\mathrm{K}2s|n'p0)$, and $S(\mathrm{K}2p0|n'p0)$, respectively (n' denotes the principal quantum number of the outer electron of the anion). If we define the functions E and F as follows:

$$E(\xi;l,m) \equiv \beta\xi_{Sl} + \beta'\xi_{S'l} - \xi_{Im} \ , \tag{22}$$

$$F(\xi,\eta;l,m,n) \equiv -\alpha\xi_{Sl} + \beta\xi_{Sm} + \beta'\xi_{S'm} + \gamma\xi_{Sn} + \gamma\eta_{Sn} \ , \tag{23}$$

then we obtain the internuclear-distance dependence of $\lambda_1^{(i)}$ and $\lambda_2^{(i)}$:

$$\lambda_X^{(i)} = E(X;i\pm1,i)/F(X,0;\min(i+2,i-2),i\pm1,i) \ , \tag{24}$$

$$\lambda_Y^{(i)} = [E(Y;i\pm1,i) - \lambda_X^{(i)}F(Y,X;\min(i+2,i-2),i\pm1,i)]/F(X,0;\min(i+2,i-2),i\pm1,i) \ , \tag{25}$$

$$\lambda_Z^{(i)} = [E(Z;i\pm1,i) - \lambda_X^{(i)}F(Z,Y;\min(i+2,i-2),i\pm1,i) - \lambda_Y^{(i)}F(Y,X;\min(i+2,i-2),i\pm1,i)]/F(X,0;\min(i+2,i-2),i\pm1,i) \ , \tag{26}$$

$$\lambda_{2X}^{(i)} = 1 - \lambda_X^{(i)}, \quad \lambda_{2Y}^{(i)} = 1 - \lambda_Y^{(i)}, \quad \text{and} \quad \lambda_{2Z}^{(i)} = 1 - \lambda_Z^{(i)}, \quad i=1,\ldots,4 \ , \tag{27}$$

where the upper sign corresponds to $i=1, 3$, and the lower one to $i=2, 4$. Here "min" means that the minimum value should be picked up out of the positive numbers in parentheses. If we replace $|I_1|$, $|S_1|$, by $|I_5|$, $|S_5|$, respectively, and remove the terms containing $|S_2|$ or $|S_3|$ in Eq. (12), then we get Eq. (13). Therefore $\lambda_1^{(5)}$ and $\lambda_2^{(5)}$ are derived by utilizing Eqs. (24)–(27) as follows:

$$\lambda_X^{(5)} = -X_{I5}/(\gamma X_{S5}) \ , \tag{28}$$

$$\lambda_Y^{(5)} = [-Y_{I5} - \lambda_X^{(5)}(\gamma Y_{S5} + \gamma X_{S5})]/(\gamma X_{S5}) \ , \tag{29}$$

$$\lambda_Z^{(5)} = [-Z_{I5} - \lambda_X^{(5)}(\gamma Z_{S5} + \gamma Y_{S5}) - \lambda_Y^{(5)}(\gamma Y_{S5} + \gamma X_{S5})]/(\gamma X_{S5}) \ , \tag{30}$$

$$\lambda_{2X}^{(5)} = 1 - \lambda_X^{(5)}, \quad \lambda_{2Y}^{(5)} = 1 - \lambda_Y^{(5)}, \quad \lambda_{2Z}^{(5)} = 1 - \lambda_Z^{(5)} \ . \tag{31}$$

For the overlap integrals with the inner-shell electrons, (which will be called S_6, S_7, ...), $\lambda_A^{(i)}$ and $\lambda_{2A}^{(i)}$ ($i=6$, 7, ..., and $A=X,Y,Z$) are determined from the similar equations (without $|S_j'|$ terms) to Eqs. (22)–(27).

Now we will first calculate the first term of the right-hand side in Eq. (4):

$$t_1(g,h,p) = 4\epsilon_p \sum_{\mu}^{(h)} \sum_{\nu}^{(g)} S_{\mu\nu} \int \frac{\Phi_\mu^*(1)\Phi_\nu(1)}{r_{1p}} d\upsilon_1 \ . \tag{32}$$

Substituting Eq. (9) into this equation, we have two terms separately. If we expand $1/r_{1p}$ in the integrand of each separated term into spherical harmonics about h for the first, while about g for the second term, then the single-center integrals alone are obtained. Secondly, combining these with the second and third terms of Eq. (4)

by means of Eqs. (5), (6) and (7), we get the final formulas

$$t(g,h,p)=\epsilon_p\left[\frac{Q_{h0}}{r_{hp}}+\frac{Q_{g0}}{r_{gp}}+\frac{Q_{h1}(3\cos^2\theta_{ghp}-1)}{r_{hp}^3}+\frac{Q_{g1}(3\cos^2\theta_{hgp}-1)}{r_{gp}^3}\right], \tag{33}$$

where

$$Q_{h0}=4\sum_{i=1}(\lambda_1^{(i)}-\tfrac{1}{2})S_i^2 , \tag{34}$$

$$Q_{g0}=4\sum_{i=1}(\lambda_2^{(i)}-\tfrac{1}{2})S_i^2 , \tag{35}$$

$$Q_{h1}=4[(\lambda_1^{(3)}-\tfrac{1}{2})S_3^2+(\lambda_1^{(4)}-\tfrac{1}{2})S_4^2-(\lambda_1^{(5)}-\tfrac{1}{2})S_5^2]G_h , \tag{36}$$

$$Q_{g1}=4[(\lambda_2^{(2)}-\tfrac{1}{2})S_2^2+(\lambda_2^{(4)}-\tfrac{1}{2})S_4^2-(\lambda_2^{(5)}-\tfrac{1}{2})S_5^2]G_g , \tag{37}$$

$$G_h\simeq\tfrac{1}{5}\int_0^\infty P_{n'hp}^2(r)r^2dr , \tag{38}$$

$$G_g\simeq\tfrac{1}{5}\int_0^\infty P_{ngp}^2(r)r^2dr . \tag{39}$$

Summation about i includes contributions from both outer- and inner-shell electrons and contains the term with S_5^2 doubly. According to Eq. (33), we note that the first two terms offer a two-point-charge model in which two overlap charges Q_{h0} and Q_{g0} are on the h and g, respectively, and the remaining small terms may be regarded as corrections. We have calculated the lattice relaxation including these correction terms. Since $\lambda_1^{(i)}+\lambda_2^{(i)}=1$ for all i, we have $Q_{h0}+Q_{g0}=0$, assuring us of electroneutrality in the whole crystal at the first-order approximation.

We shall investigate the distance dependence of $t(g,h,p)$ in which ϵ's are taken to the extent of the second order of ion displacements. In Tables VI and VII in RI, these dependences of Q_{h0}, Q_{g0} and Q_{h1}, Q_{g1} have already been calculated in terms of ξ_i, η_i, ζ_i and $\alpha_i, \beta_i, \gamma_i$ $(i=1,2)$, respectively, where Q_{h0}, Q_{g0} and Q_{h1}, Q_{g1} are multiplied by e^2/R_0 and $e^2a_H^2/R_0^3$, respectively.[24] If the inner-shell electrons are omitted in the calculation of Q_{h0} (or Q_{g0}), the relative errors of ξ_1 (or ξ_2), η_1 (or η_2), and ζ_1 (or ζ_2) amount to about 0.71, 0.75, and 0.78% for $1s$ electrons in Na^+ and to 1.78, 1.94, and 2.28% for $2s$ and $2p$ electrons in K^+, respectively.

According to Eq. (33), it is noted that the dependence of $T(g,h)$ upon the nearest-neighbor distance will consist of three parts:

(i) $\Delta T_1(g,h)$: The potentials arising from the p ion are constant and four charges consist of linear and quadratic terms in ϵ. Therefore,

$$\Delta T_1(g,h)=-(\kappa-1)\Delta(Q_{g0}-Q_{h0})+2\Delta(Q_{g1}-Q_{h1}) , \tag{40}$$

where $\kappa=1.747\,564$ is the Madelung constant referred to R_0 for the face-centered-cubic lattice[25]; and the variation of charges, Δ's, are composed of the terms proportional to ϵ and ϵ^2. By using Table II and abbreviations $\partial\Delta E_{T1}/\partial a=E_a$, etc., where $\Delta E_{T1}=\frac{1}{2}\sum'_{g,h}\Delta T_1(g,h)$, we obtain the next equations:

$$\begin{aligned}
E_a&=l_0'-l_0/4+(2m_0'+l_0+m_0/2)a-l_0b-m_0d ,\\
E_b&=-l_0a+4(l_0+m_0)b-2l_0c-4m_0e-l_0f ,\\
E_c&=-2l_0b+4(l_0+m_0)c-4m_0g-2l_0h ,\\
E_d&=-m_0a+4(l_0+m_0)d-4l_0e-3m_0j ,\\
E_e&=-4m_0b-4l_0d+16(l_0+m_0)e-8l_0g-4l_0i-12m_0m ,\\
E_f&=-l_0b+4(l_0+m_0)f-2l_0h-4m_0i-l_0n ,\\
E_g&=-4m_0c-8l_0e+16(l_0+m_0)g-8l_0k-12m_0p ,\\
E_h&=-2l_0c-2l_0f+8(l_0+m_0)h-8m_0k-2l_0l-2l_0p ,\\
E_i&=-4l_0e-4m_0f+16(l_0+m_0)i-8l_0k-12m_0r-4l_0s ,\\
E_j&=-3m_0d+9(l_0+m_0)j-9l_0m-6m_0u ,\\
E_k&=-8l_0g-8m_0h-8l_0i+32(l_0+m_0)k-8l_0q-8(l_0+3m_0)t ,\\
E_l&=-2l_0h+4(l_0+m_0)l-4m_0q-2l_0t ,\\
E_m&=-12m_0e-9l_0j+36(l_0+m_0)m-18l_0p-9l_0r ,\\
E_n&=-l_0f+4(l_0+m_0)n-2l_0p-4m_0s ,\\
E_p&=-12m_0g-2l_0h-18l_0m-2l_0n+44(l_0+m_0)p-4(5l_0+2m_0)t ,\\
E_q&=-8l_0k-4m_0l+16(l_0+m_0)q ,\\
E_r&=-12m_0i-9l_0m+36(l_0+m_0)r-18l_0t ,\\
E_s&=-4l_0i-4m_0n+16(l_0+m_0)s-8l_0t ,\\
E_t&=-8(l_0+3m_0)k-2l_0l-4(5l_0+2m_0)p-18l_0r-8l_0s+112(l_0+m_0)t ,\\
E_u&=-6m_0j+16(l_0+m_0)u .
\end{aligned} \tag{41}$$

Here only the first term in Eq. (40) was treated and

$$l_0' = -6(\kappa-1)(\eta_2-\eta_1), \quad m_0' = -6(\kappa-1)(\zeta_2-\zeta_1) \ , \tag{42}$$

for the impurity-host ion pair, while, about the host-host ion pair,

$$l_0 = -24(\kappa-1)(\eta_2-\eta_1), \quad m_0 = -24(\kappa-1)(\zeta_2-\zeta_1) \ . \tag{43}$$

Here η_1, ζ_1 and η_2, ζ_2 satisfy Eqs. (19) and (20) in RI, respectively.

(ii) $\Delta T_2(g,h)$: Both the charges and the potentials originating in the p ion have the linear terms with respect to ϵ.

(iii) $\Delta T_3(g,h)$: This term is a combination between four charges with 0th order of ϵ and potentials coming from the p ion which are the first or second order of ϵ.

The calculation on ΔE_T of the overlap integrals between the second-neighbor anions was performed similarly. In this case, however, Q_{h0} and Q_{g0} vanish for the host-host ion pairs because $\lambda_1^{(i)} = \lambda_2^{(i)} = \frac{1}{2}$ for all i in these pairs. The potentials in ΔT_2 and ΔT_3 for the nearest- and next-nearest-neighbor overlaps were calculated by a computer (ACOS series 77 NEAC-S800).[26]

V. RAA MODEL

Another method treating the first term in Eq. (4) was developed by Ra,[12] Abarenkov and Antonova[13] as referred in the Introduction.

The charge distribution

$$\rho(1) = 4 \sum_{\mu}^{(h)} \sum_{\nu}^{(g)} S_{\mu\nu} \Phi_{\mu}^{*}(1) \Phi_{\nu}(1) \tag{44}$$

is replaced with a point charge on the electric center of gravity (ECG) of the distribution $\rho(1)$ chosen to provide the same "charge" and "dipole moment." By means of this approximation Eq. (4) will be written in the form

$$t(g,h,p) = \epsilon_p \left(\frac{W_{gh}(g,h)}{r_{gh,p}} + \frac{W_0(g,h)}{r_{hp}} + \frac{W_0(g,h)}{r_{gp}} + \frac{W_h(3\cos^2\theta_{ghp}-1)}{r_{hp}^3} + \frac{W_g(3\cos^2\theta_{hgp}-1)}{r_{gp}^3} \right) , \tag{45}$$

where

$$W_{gh}(g,h) = 4 \sum_i S_i^2 \ , \tag{46}$$

$$W_0(g,h) = -2 \sum_i S_i^2 = -2M_0(g,h) \ , \tag{47}$$

$$W_h = -2M_h(g,h) \ , \tag{48}$$

$$W_g = -2M_g(g,h), \quad i = 1, \ldots, 7, \ldots , \tag{49}$$

and $r_{gh,p}$ represents the distance between the p ion and the ECG of the charge distribution $\rho(1)$. A three-point-charge model will be produced from the first three terms of Eq. (45), in which W_{gh} and W_0's are on the ECG and on both sites of the overlapping ion pair, respectively, provided that the other terms are simply regarded as corrections. The internuclear-distance dependence of the charges W_{gh} (accordingly W_0) and W_h, W_g were already given as λ, μ, ν and ρ_i, σ_i, π_i $(i = 1, 2)$ in Tables VI and VII of RI, where W_{gh} and W_h, W_g were multiplied by e^2/R_0 and $e^2 a_H^2/R_0^3$, respectively.[24]

From the Eqs. (15) and (16) we have the first-order equations with respect to ϵ in the form

$$|I_i| = X_{Ii} + Y_{Ii}\epsilon \ , \tag{50}$$

$$|S_i| = X_{Si} + Y_{Si}\epsilon \ , \tag{51}$$

then

$$S_i^2 = X_{Si}^2 + 2X_{Si}Y_{Si}\epsilon \ , \tag{52}$$

$$|I_i S_i| = X_{Ii}X_{Si} + (X_{Ii}Y_{Si} + Y_{Ii}X_{Si})\epsilon, \quad i = 1, \ldots, 6, \ldots \ , \tag{53}$$

When the origin is taken at the anion site of the nearest-neighbor overlap-ion pair, the distance from the origin to the ECG, r_G will be

$$r_G = 1 - \left[\frac{1}{a_0} \sum_i \left(S_i \int \Phi_{\mu} r_i \cos\theta_i \Phi_{\nu} d\upsilon_1 \right) \right] \Big/ \left(\sum_i S_i^2 \right) \ , \tag{54}$$

in units of the nearest-neighbor distance. Since these integrals are exactly I_i, we obtain the distance dependence of r_G:

$$r_G = l_G + m_G\epsilon \ , \tag{55}$$

$$l_G = 1 - \left(\sum_i X_{Ii}X_{Si} \right) \Big/ \left(a_0 \sum_i X_{Si}^2 \right) \ , \tag{56}$$

$$m_G = \frac{1}{a_0} \left(\sum_i X_{Ii}X_{Si} \Big/ \sum_i X_{Si}^2 \right) \left| \left(\sum_i 2X_{Si}Y_{Si} \right) \Big/ \sum_i X_{Si}^2 - \sum_i (X_{Ii}Y_{Si} + Y_{Ii}X_{Si}) \Big/ \left(\sum_i X_{Ii}X_{Si} \right) \right| \ . \tag{57}$$

For the second-neighbor overlaps the equations similar to Eqs. (45)–(57) will be also written, however, it may be important to examine if the origins of r_G and I_i coincide with each other. The calculated values of l_G and m_G for the nearest- and next-nearest-neighbor overlaps are shown in Table III. We have computed both overlap effects carefully including the distance dependence of correction terms. As in the LST model, $\Delta T(g,h)$ will consist of three parts $\Delta T_1(g,h)$, $\Delta T_2(g,h)$, and $\Delta T_3(g,h)$. Summing up Eq. (45) about p in order to get $\Delta T_1(g,h)$, the second and third terms will cancel each other because of the opposite signs and same absolute values of the Madelung potentials on both sites of the nearest-neighbor overlapping ion pair, therefore the first term will be the main term in the $\Delta T_1(g,h)$. If we write down W_{gh} in the form

$$\frac{e^2}{R_0} W_{gh}(g,h) = E_X + D_X\epsilon + C_X\epsilon^2 \tag{58}$$

for the impurity-host ion pair, and

$$\frac{e^2}{R_0} W_{gh}(g,h) = E_y + D_y\epsilon + C_Y\epsilon^2 \tag{59}$$

for the host-host ion pair, then Eqs. (42) and (43) will be replaced by

$$l_0' = 6\kappa_G' D_x, \quad m_0' = 6\kappa_G' C_x \ , \tag{60}$$

$$l_0 = 24\kappa_G' D_y, \quad m_0 = 24\kappa_G' C_y, \tag{61}$$

where κ_G' represents the Madelung potential at the ECG except the contribution from overlap-pair ions in order to exclude the two-body potential. Therefore, the κ_G' corresponds to $\kappa - 1$ in the LST model. And then Eqs. (41) still hold in the case of the nearest-neighbor overlaps of RAA model. The κ_G' in the crystals under study was calculated including the contributions from 120^3 ions as shown in Table VIII of RI.[16]

TABLE III. Electric center of gravity of charge distribution, $\rho(1) = \sum_{\mu}^{(h)} \sum_{\nu}^{(g)} S_{\mu\nu} \Phi_{\mu}^{*}(1) \Phi_{\nu}(1)$. The distance from the origin to the electric center of gravity for the nearest-neighbor overlaps is given by $r_G = l_G + m_G\epsilon$ (ϵ's are shown in Table II) in units of R_0 where the origin is taken at the anion site of the overlap pair, and that for the second-neighbor overlaps is $r_G = \sqrt{2}(l_G + m_G b)$ in units of R_0 where the origin is taken at the impurity anion site.

Neighbor	Overlap pair	l_G	m_G
Nearest neighbor	Na-F in NaF	0.7247	0.1658
	Na-F in KF	0.7448	0.0947
	K-F in KF	0.6447	0.3990
	K-F in NaF	0.6617	0.5967
	Na-Cl in NaCl	0.7686	0.0516
	Na-Cl in NaBr	0.7788	0.0430
	Na-Br in NaBr	0.7882	0.0528
	Na-Br in NaCl	0.7793	0.0666
	Na-Br in KBr	0.8044	0.0352
	K-Cl in KCl	0.6563	0.1307
	K-Cl in NaCl	0.6338	0.1708
	K-Cl in KBr	0.6668	0.1152
	K-Br in KBr	0.6806	0.1340
	Na-I in NaI	0.8104	0.0370
	Na-Br in NaI	0.8005	0.0388
	Na-Cl in NaI	0.7924	0.0357
	Na-I in NaCl	0.7917	0.0841
	Na-I in NaBr	0.7991	0.0634
Second neighbor	Cl-Br in NaCl	0.5613	0.5574
	Br-Cl in NaBr	0.4445	0.5095
	Br-Cl in KBr	0.4500	0.4948
	Cl-I in NaCl	0.5732	0.5171
	I-Cl in NaI	0.4319	0.4602
	I-Br in NaI	0.4414	0.5014
	Br-I in NaBr	0.5605	0.5101

The potential calculations of $\Delta T_2(g,h)$ and $\Delta T_3(g,h)$ are very complicated; however, we note that the first three terms are put together in the form

$$\epsilon_p\left[\frac{1}{r_{gh,p}}-\frac{1}{2}\left(\frac{1}{r_{hp}}+\frac{1}{r_{gp}}\right)\right]4\sum_i S_i^2 \ , \tag{62}$$

and the computations of $\Delta T_2(g,h)$ and $\Delta T_3(g,h)$ will become comparatively simpler. We have calculated the potentials of ΔT_2 and ΔT_3 in both the first- and second-neighbor overlaps by the computer.[26]

The LST model generally has a property that calculations of potentials from the p ion will be fairly short, but those on charges are troublesome as seen in the last section. On the other hand, in the RAA model the charges are obtained much easier, while the computations of potentials are very tedious owing to containing the ECG. Generally speaking, the LST model is simpler than the RAA one.

VI. ELECTRIC FIELD GRADIENTS

Das and Dick investigated early the EFG in the impurity-doped ionic crystals in a different way from ours and obtained a general form of EFG-tensor components at a point with Cartesian coordinates (x_1,x_2,x_3) relative to the point dipole M whose direction cosines are (l_1,l_2,l_3).[3,4] The point dipoles of the displaced ions will consist of the displacements of the ions and the electronic polarizations. We have extended their point dipoles as follows:

$$\begin{aligned}
&M_A=qa+\mu_A,\quad M_B=-q2^{1/2}b+\mu_B,\quad M_C=q3^{1/2}c+\mu_C \ ,\\
&M_D=-q2d+\mu_D,\quad l_EM_E=q2e+\mu_{EX},\quad m_EM_E=qf+\mu_{EY} \ ,\\
&l_GM_G=-q2g+\mu_{GX},\quad m_GM_G=-gh+\mu_{GY},\quad M_I=-q8^{1/2}i+\mu_I \ ,\\
&M_J=q3j+\mu_J,\quad m_KM_K=q2k+\mu_{KY},\quad n_KM_K=ql+\mu_{KZ} \ ,\\
&l_MM_M=-q3m+\mu_{MX},\quad m_MM_M=-qn+\mu_{MY},\quad l_PM_P=q3p \ ,\\
&m_PM_P=qp,\quad M_Q=-q(12)^{1/2}q,\quad l_RM_R=q3r \ ,\\
&m_RM_R=q2s,\quad l_TM_T=-q3t,\quad m_TM_T=-q2t \ ,\\
&n_TM_T=-qt,\quad M_U=-q4u \ ,
\end{aligned} \tag{63}$$

where l_i, m_i, and n_i stand for the direction cosines of M_i relative to the crystal axes and μ_i's are the electronic polarizations of the ions arising from the electric fields at their sites produced after impurity substitution, and $q=+1$ or -1 are for the case of the anion or cation impurity, respectively. The μ_i of the i ion was evaluated by an equation:

$$\vec{\mu}_i=\frac{\alpha_i}{R_0^2}\sum_k{}'\frac{Q_k\vec{r}_{ki}}{r_{ki}^3} \ , \tag{64}$$

where α_i, Q_k, and r_{ki} represent the polarizability of the i ion, the charge of the k ion in units of e and the distance between the i and k ion, respectively. Here summation goes over all 256 ions including the impurity and excluding the i ion. In Eqs. (63) we have ignored $\mu_P,\ldots,\mu_U$ because of very small quantities. By using Das and Dick's general form we get the EFG components at (1,0,0), (1,1,0), (1,1,1), (2,0,0), (2,1,0), and (4,0,0) sites in units of $3e/R_0^3$.[27]

Every point dipole M_j except M_i in Eq. (63) will produce the EFG directly at the nuclear site of the i ion in question ($i=A,B,\ldots,U$). Distortions of the electron shells in this i ion originating in the M_j also will yield the EFG at the same nuclear site indirectly. The latter called the antishielding effect is much larger than the former and we have $eq^i=E_{ij}(1-\gamma_\infty)3e/R_0^3$ as the combined EFG, where E_{ij}'s are the direct EFG (the subscripts of E, i, and j represent the crystal axes) and $1-\gamma_\infty$ expresses the Sternheimer antishielding factor. Another electron-shell distortion in the i ion will be produced by means of the displacement of the i ion itself due to impurity substitution. This distortion also will give rise to the EFG at the same nuclear site in the i ion. Since this is a difficult problem to study, no one has ever investigated this effect on the EFG, therefore we have adopted an approximation semiempirically in which it is assumed that the distortion and accordingly the EFG are proportional to the displacement of the concerned i ion. This type of EFG's will be called eq^{el} hereafter. The proportionality constant k will be appropriate to the concerned ion and determined so that the calculated EFG may coincide with the experimental one, then this constant is applied to the same ion in the other crystals.

For the ion at (1,1,0) site thus we have a secular equation:

$$\begin{vmatrix} p+r-x, & q, & 0 \\ q, & p+r-x, & 0 \\ 0, & 0, & -2p-2r-x \end{vmatrix}=0 \ , \tag{65}$$

where

$$p = E_{xx}(1-\gamma_\infty)3e/R_0^3, \quad q = E_{xy}(1-\gamma_\infty)3e/R_0^3 \quad , (66)$$

and

$$r = kb \ (k; \text{ constant mentioned above}). \qquad (67)$$

Solving this equation we obtain the principal values of the EFG:

$$\frac{3e^2}{R_0^3}(1-\gamma_\infty)(E_{xx}+E_{xy})+kb \quad \text{for } (1,1,0),$$

$$\frac{3e^2}{R_0^3}(1-\gamma_\infty)(E_{xx}-E_{xy})+kb \quad \text{for } (1,\bar{1},0),$$

$$-\frac{6e^2}{R_0^3}(1-\gamma_\infty)E_{xx}-2kb \quad \text{for } (0,0,1),$$

[(i,j,k) expresses the direction cosines of the principal axes], because of 45° rotation of the x and y crystal axes about z axis. The principal values and the asymmetry parameter, η are defined as[28]

$$|E_{x'x'}| \leq |E_{y'y'}| \leq |E_{z'z'}|, \quad E_{z'z'} \equiv eq \quad , \qquad (68)$$

$$\eta = (E_{x'x'} - E_{y'y'})/E_{z'z'}, \quad 0 \leq \eta \leq 1 \quad , \qquad (69)$$

where x', y', and z' represent the principal axes. Therefore we will classify the types of EFG tensors on the (1,1,0) site according to the direction cosines of principal axes relative to the crystal axes:

$$A\begin{cases} x';(0,0,1) \\ y';(1,\bar{1},0), \\ z';(1,1,0) \end{cases} \quad B\begin{cases} x';(1,\bar{1},0) \\ y';(0,0,1), \\ z';(1,1,0) \end{cases} \quad C\begin{cases} x';(1,1,0) \\ y';(0,0,1), \\ z';(1,\bar{1},0) \end{cases}$$

$$D\begin{cases} x';(0,0,1) \\ y';(1,1,0), \\ z';(1,\bar{1},0) \end{cases} \quad E\begin{cases} x';(1,1,0) \\ y';(1,\bar{1},0), \\ z';(0,0,1) \end{cases} \quad F\begin{cases} x';(1,\bar{1},0) \\ y';(1,1,0) \\ z';(0,0,1) \end{cases} .$$

Thus the definite assignment of the tensor types can be carried out by calculation, but this is impossible from the experiments on the first-order splittings of the NMR lines as noted in RII since we can get merely information that some crystal has the type A or D and another one possesses B or C, etc., from the experimental data. A crystal of type E or F has never been found empirically.

For the ion at the (2,1,0) site a similar procedure will be applied and we then obtain the principal values of the EFG:

$$\{p+q+t+u \pm [(p-q+t-u)^2+4s^2]^{1/2}\}/2$$

and

$$r-t-u \quad ,$$

with a rotation about z axis whose angle will be

$$\phi = \tfrac{1}{2}\tan^{-1}[(2s)/(p-q+t-u)] \quad , \qquad (70)$$

where

$$p = E_{xx}(1-\gamma_\infty)3e/R_0^3, \quad q = E_{yy}(1-\gamma_\infty)3e/R_0^3 \quad , (71)$$

$$r = E_{zz}(1-\gamma_\infty)3e/R_0^3, \quad s = E_{xy}(1-\gamma_\infty)3e/R_0^3 \quad , (72)$$

$$t = k2e, \quad u = k'f \quad , \qquad (73)$$

and

$$p+q+r=0. \qquad (74)$$

Here $2e$ and f are the displacements of the (2,1,0) ion in the x and y directions as shown on Table I and k and k' are the proportionality constants of the x and y directions, respectively.

For the (1,0,0) and (2,0,0) sites we have also evaluated eq^i and eq^{el} likewise, while the ion on the (1,1,1) site has no eq^{el} owing to the symmetry of this lattice site.

As shown in the next section the evaluated quantities establishing an EFG tensor, i.e., eq, η and the type of tensor compare quite well with the experimental ones. For the crystals containing potassium ions, however, agreement is very poor, for instance, in NaCl-K and NaF-K, since in these crystals the overlap integrals for the impurity-host ion pair are much larger than those of the other crystals as shown in Table VI of RI. This is due to the fairly large orbitals of valence electrons in the potassium ion at comparatively small ionic distances. Covalent bonding between these ions will be expected in which an electron on the p orbital of the anion is momentarily transferred to the orbital of the neighboring potassium ion. Provided that the degree of covalency λ is defined as a rate in which the covalent-bonding state of an overlapping pair is mixed with the ionic state, λ will be proportional to the probability of this transition and written in the form

$$\lambda \propto A_c \exp(-R/\rho_c) \simeq \lambda_0\left[1-\frac{R_0}{\rho_c}\epsilon+\frac{R_0^2}{2\rho_c^2}\epsilon^2\right] \quad , \qquad (75)$$

with

$$\lambda_0 = A_c \exp(-R_0/\rho_c) \qquad (76)$$

and

$$R = R_0(1+\epsilon) \quad . \qquad (77)$$

Accordingly we can express the dependence of λ on the internuclear distance, with λ_0 and ρ_c. Since the covalency will be produced from the overlap integral between the valence-electron orbital of the anion and the orbital of the excited state of a potassium ion, this integral will be much larger than that of the valence electron of K ions, we may anticipate that saturation of λ on the internuclear distance occurs in some crystals. Consequently we have adopted one of the following three types for each crystal containing

K^+ ion:

(i) Perfect saturation: Owing to the extremely large overlap, λ has no dependence on the internuclear distance. Therefore the second and third terms in Eq. (75) are omitted.

(ii) Linear dependence on ϵ: Third term is vanishing.

(iii) No saturation: Eq. (75) is valid. Regarding the transferred electronic charge in the orbital of the potassium ion and the missing one in that of the anion as the negative and positive point charges on each lattice sites, respectively, we can apply the same process of potential-energy calculations as shown in the last section, for the superposed point charges on both sites of the overlapping pair ion which originate in both overlap and covalency.

VII. RESULTS

A. Lattice relaxation

In Secs. IV and V two different ways of calculating ΔE_T were described in detail. Thus, calculating the changes of total potential energy in Eq. (1) after impurity substitution and solving 20 linear equations with respect to the displacements of the ion obtained from differentiation of them, the lattice-relaxation parameters in twelve impurity-doped ionic crystals have been evaluated by using the computer.[26]

The relaxation parameters calculated by four different methods are listed in Table IV, and those obtained from taking both overlap and covalency into consideration for crystals with potassium ions are given in Table V. In Table IV, the third, seventh,

TABLE IV. Lattice-relaxation parameters obtained from four different methods. The third, seventh, and fourth, eighth columns represent the calculations without the three-body potentials by us and by Douglas (Ref. 6), respectively.

Crystal		LST	RAA	No ΔE_T	No ΔE_T (DG)		LST	RAA	No ΔE_T	No ΔE_T (DG)
NaCl-Br	$a \times 10^3$	+21.91	+22.16	+23.47	+24.51	$b \times 10^3$	+6.83	+5.00	+5.76	+6.10
	$c \times 10^3$	+0.18	−1.65	−0.57	−0.64	$d \times 10^3$	+0.34	+1.37	+2.23	+2.06
	$e \times 10^3$	+1.33	+1.52	+1.57	+1.42	$f \times 10^3$	+3.50	+3.29	+2.94	+2.85
	$g \times 10^3$	+0.92	+0.64	+0.63	+0.51	$h \times 10^3$	+0.71	+0.25	+0.20	+0.18
	$i \times 10^3$	+1.01	+0.66	+0.91	+0.83	$j \times 10^3$	−0.07	−0.05	+0.41	+0.27
	$k \times 10^3$	+0.27	−0.06	+0.08		$l \times 10^3$	+0.52	+0.45	+0.25	
	$m \times 10^3$	+0.11	+0.22	+0.34		$n \times 10^3$	+0.41	+0.57	+0.58	
	$p \times 10^3$	+0.24	+0.27	+0.24		$q \times 10^3$	+0.17	+0.08	+0.06	
	$r \times 10^3$	+0.22	+0.22	+0.26		$s \times 10^3$	+0.44	+0.43	+0.38	
	$t \times 10^3$	+0.15	+0.09	+0.09		$u \times 10^3$	−0.03	+0.01	+0.06	
NaBr-Cl	$a \times 10^3$	−20.14	−19.72	−22.68	−21.58	$b \times 10^3$	−5.84	−4.35	−5.26	−5.14
	$c \times 10^3$	−0.02	+1.27	+0.58	+0.52	$d \times 10^3$	−0.78	−1.41	−2.39	−1.34
	$e \times 10^3$	−1.27	−1.32	−1.49	−1.14	$f \times 10^3$	−2.96	−2.70	−2.66	−2.32
	$g \times 10^3$	−0.77	−0.53	−0.55	−0.42	$h \times 10^3$	−0.52	−0.19	−0.15	−0.16
	$i \times 10^3$	−0.87	−0.60	−0.83	−0.68	$j \times 10^3$	−0.03	−0.07	−0.48	−0.21
	$k \times 10^3$	−0.21	+0.03	−0.06		$l \times 10^3$	−0.39	−0.33	−0.21	
	$m \times 10^3$	−0.16	−0.22	−0.35		$n \times 10^3$	−0.43	−0.48	−0.56	
	$p \times 10^3$	−0.23	−0.23	−0.22		$q \times 10^3$	−0.12	−0.07	−0.05	
	$r \times 10^3$	−0.21	−0.19	−0.24		$s \times 10^3$	−0.38	−0.35	−0.34	
	$t \times 10^3$	−0.13	−0.07	−0.08		$u \times 10^3$	+0.01	−0.02	−0.07	
KBr-Cl	$a \times 10^3$	−14.03	−16.43	−21.40	−19.89	$b \times 10^3$	−3.93	−1.83	−3.81	−3.56
	$c \times 10^3$	−0.03	+1.84	+0.70	+0.62	$d \times 10^3$	−1.05	−2.34	−3.91	−2.87
	$e \times 10^3$	−0.99	−1.19	−1.38	−1.01	$f \times 10^3$	−1.79	−1.40	−1.77	−1.49
	$g \times 10^3$	−0.51	−0.14	−0.22	−0.15	$h \times 10^3$	−0.22	+0.18	+0.13	+0.01
	$i \times 10^3$	−0.58	−0.28	−0.60	−0.48	$j \times 10^3$	−0.13	−0.58	−1.05	−0.60
	$k \times 10^3$	−0.13	+0.25	+0.04		$l \times 10^3$	−0.15	−0.07	−0.05	
	$m \times 10^3$	−0.18	−0.25	−0.44		$n \times 10^3$	−0.36	−0.26	−0.53	
	$p \times 10^3$	−0.18	−0.15	−0.12		$q \times 10^3$	−0.06	−0.02	−0.00	
	$r \times 10^3$	−0.15	−0.11	−0.20		$s \times 10^3$	−0.23	−0.26	−0.24	
	$t \times 10^3$	−0.07	−0.00	−0.01		$u \times 10^3$	−0.01	−0.11	−0.24	

TABLE IV *(Continued).*

Crystal		LST	RAA	No ΔE_T	No ΔE_T (DG)		LST	RAA	No ΔE_T	No ΔE_T (DG)
	$a \times 10^3$	+51.39	+52.87	+53.92	+63.87	$b \times 10^3$	+16.66	+12.37	+13.74	+16.31
	$c \times 10^3$	+0.76	−3.57	−1.06	−1.64	$d \times 10^3$	+0.60	+3.36	+5.06	+6.77
	$e \times 10^3$	+3.17	+3.69	+3.67	+3.95	$f \times 10^3$	+8.37	+7.91	+6.85	+7.61
	$g \times 10^3$	+2.22	+1.58	+1.51	+1.31	$h \times 10^3$	+1.79	+0.68	+0.53	+0.46
	$i \times 10^3$	+2.44	+1.63	+2.16	+2.25	$j \times 10^3$	−0.19	−0.11	+0.94	+0.87
NaCl-I	$k \times 10^3$	+0.68	−0.09	+0.23		$l \times 10^3$	+1.26	+1.08	+0.58	
	$m \times 10^3$	+0.26	+0.53	+0.80		$n \times 10^3$	+0.94	+1.38	+1.33	
	$p \times 10^3$	+0.57	+0.67	+0.57		$q \times 10^3$	+0.41	+0.20	+0.14	
	$r \times 10^3$	+0.52	+0.53	+0.61		$s \times 10^3$	+1.07	+1.04	+0.88	
	$t \times 10^3$	+0.37	+0.22	+0.22		$u \times 10^3$	−0.06	+0.03	+0.13	
	$a \times 10^3$	−42.62	−41.06	−49.59	−46.79	$b \times 10^3$	−11.63	−8.99	−10.99	−10.69
	$c \times 10^3$	+0.10	+2.09	+1.22	+1.01	$d \times 10^3$	−2.57	−3.41	−5.74	−2.46
	$e \times 10^3$	−2.76	−2.71	−3.22	−2.33	$f \times 10^3$	−5.72	−5.15	−5.40	−4.64
	$g \times 10^3$	−1.48	−1.04	−1.11	−0.87	$h \times 10^3$	−0.88	−0.37	−0.26	−0.38
	$i \times 10^3$	−1.75	−1.27	−1.72	−1.39	$j \times 10^3$	−0.31	−0.40	−1.26	−0.45
NaI-Cl	$k \times 10^3$	−0.37	+0.00	−0.12		$l \times 10^3$	−0.65	−0.56	−0.38	
	$m \times 10^3$	−0.46	−0.51	−0.80		$n \times 10^3$	−0.95	−0.95	−1.21	
	$p \times 10^3$	−0.49	−0.45	−0.46		$q \times 10^3$	−0.21	−0.13	−0.09	
	$r \times 10^3$	−0.45	−0.40	−0.52		$s \times 10^3$	−0.73	−0.66	−0.69	
	$t \times 10^3$	−0.24	−0.14	−0.16		$u \times 10^3$	−0.01	−0.06	−0.21	
	$a \times 10^3$	−27.11	−26.55	−30.72	−29.12	$b \times 10^3$	−7.44	−5.83	−6.87	−6.74
	$c \times 10^3$	+0.04	+1.34	+0.73	+0.62	$d \times 10^3$	−1.63	−2.21	−3.55	−1.85
	$e \times 10^3$	−1.76	−1.76	−2.01	−1.51	$f \times 10^3$	−3.65	−3.33	−3.36	−2.93
	$g \times 10^3$	−0.95	−0.67	−0.70	−0.54	$h \times 10^3$	−0.56	−0.24	−0.17	−0.24
	$i \times 10^3$	−1.12	−0.82	−1.08	−0.88	$j \times 10^3$	−0.20	−0.26	−0.78	−0.33
NaI-Br	$k \times 10^3$	−0.24	−0.00	−0.08		$l \times 10^3$	−0.41	−0.36	−0.24	
	$m \times 10^3$	−0.29	−0.33	−0.50		$n \times 10^3$	−0.61	−0.61	−0.75	
	$p \times 10^3$	−0.31	−0.29	−0.29		$q \times 10^3$	−0.13	−0.08	−0.06	
	$r \times 10^3$	−0.28	−0.26	−0.32		$s \times 10^3$	−0.46	−0.42	−0.43	
	$t \times 10^3$	−0.15	−0.09	−0.10		$u \times 10^3$	−0.01	−0.04	−0.13	
	$a \times 10^3$	+30.22	+30.78	+32.19	+34.85	$b \times 10^3$	+9.14	+7.05	+7.82	+8.64
	$c \times 10^3$	+0.22	−1.78	−0.67	−0.79	$d \times 10^3$	+1.09	+2.25	+3.37	+3.40
	$e \times 10^3$	+1.94	+2.10	+2.17	+2.07	$f \times 10^3$	+4.53	+4.25	+3.84	+3.90
	$g \times 10^3$	+1.20	+0.86	+0.83	+0.68	$h \times 10^3$	+0.84	+0.34	+0.25	+0.27
	$i \times 10^3$	+1.36	+0.96	+1.23	+1.17	$j \times 10^3$	+0.04	+0.12	+0.68	+0.50
NaBr-I	$k \times 10^3$	+0.34	−0.02	+0.11		$l \times 10^3$	+0.60	+0.52	+0.30	
	$m \times 10^3$	+0.24	+0.35	+0.51		$n \times 10^3$	+0.63	+0.76	+0.80	
	$p \times 10^3$	+0.35	+0.36	+0.33		$q \times 10^3$	+0.20	+0.11	+0.07	
	$r \times 10^3$	+0.32	+0.31	+0.36		$s \times 10^3$	+0.58	+0.55	+0.49	
	$t \times 10^3$	+0.20	+0.12	+0.12		$u \times 10^3$	−0.02	+0.03	+0.10	
	$a \times 10^3$	+33.60	+53.99	+50.39	+55.25	$b \times 10^3$	+11.77	+14.35	+11.71	+12.42
	$c \times 10^3$	−0.14	−0.79	−1.61	−2.46	$d \times 10^3$	−0.71	+5.86	+5.55	+6.85
	$e \times 10^3$	+2.14	+3.64	+3.44	+3.36	$f \times 10^3$	+6.11	+6.54	+6.67	+6.47
	$g \times 10^3$	+1.64	+1.34	+1.27	+0.94	$h \times 10^3$	+1.13	−0.06	+0.30	−0.05
	$i \times 10^3$	+1.71	+2.44	+1.95	+1.80	$j \times 10^3$	−0.26	+1.27	+0.78	+0.59
NaCl-K	$k \times 10^3$	+0.41	+0.21	+0.15		$l \times 10^3$	+0.96	+0.27	+0.66	
	$m \times 10^3$	+0.14	+0.96	+0.79		$n \times 10^3$	+0.51	+1.30	+1.51	
	$p \times 10^3$	+0.38	+0.52	+0.53		$q \times 10^3$	+0.28	−0.01	+0.13	
	$r \times 10^3$	+0.35	+0.60	+0.58		$s \times 10^3$	+0.75	+0.76	+0.84	
	$t \times 10^3$	+0.25	+0.16	+0.18		$u \times 10^3$	−0.05	+0.25	+0.12	

TABLE IV *(Continued).*

Crystal		LST	RAA	No ΔE_T	No ΔE_T (DG)		LST	RAA	No ΔE_T	No ΔE_T (DG)
KF-Na	$a \times 10^3$	−33.19	−64.63	−61.11	−53.08	$b \times 10^3$	−11.43	−16.11	−12.76	−11.23
	$c \times 10^3$	−0.63	−1.12	+2.46	+1.88	$d \times 10^3$	+0.60	−11.12	−8.65	−4.59
	$e \times 10^3$	−1.97	−3.85	−4.15	−2.81	$f \times 10^3$	−5.86	−6.98	−6.85	−5.22
	$g \times 10^3$	−1.66	−1.15	−1.09	−0.77	$h \times 10^3$	−1.33	+0.72	+0.19	+0.01
	$i \times 10^3$	−1.61	−3.11	−2.15	−1.58	$j \times 10^3$	+0.38	−1.90	−1.76	−0.67
	$k \times 10^3$	−0.53	−0.46	+0.02		$l \times 10^3$	−0.97	+0.14	−0.41	
	$m \times 10^3$	−0.03	−1.44	−1.14		$n \times 10^3$	−0.64	−2.47	−1.76	
	$p \times 10^3$	−0.35	−0.50	−0.53		$q \times 10^3$	−0.32	+0.38	−0.06	
	$r \times 10^3$	−0.29	−0.62	−0.67		$s \times 10^3$	−0.74	−0.73	−0.91	
	$t \times 10^3$	−0.26	−0.15	−0.12		$u \times 10^3$	+0.06	−0.40	−0.34	
NaF-Li	$a \times 10^3$	−56.98	−56.02	−57.36	−46.79	$b \times 10^3$	−23.06	−15.71	−15.74	−12.80
	$c \times 10^3$	−3.30	−0.50	+1.93	+1.64	$d \times 10^3$	+8.13	−4.23	−2.15	+0.42
	$e \times 10^3$	−2.00	−3.40	−3.74	−2.34	$f \times 10^3$	−12.44	−7.27	−9.25	−6.36
	$g \times 10^3$	−3.21	−1.74	−2.09	−1.39	$h \times 10^3$	−5.11	−0.40	−1.12	−0.31
	$i \times 10^3$	−2.91	−2.86	−2.50	−1.59	$j \times 10^3$	+1.26	−0.74	+0.06	+0.15
	$k \times 10^3$	−1.15	−0.51	−0.30		$l \times 10^3$	−3.67	−0.44	−1.33	
	$m \times 10^3$	+1.06	−0.70	−0.48		$n \times 10^3$	+1.00	−1.33	−1.30	
	$p \times 10^3$	+0.01	−0.55	−0.63		$q \times 10^3$	−1.03	−0.00	−0.28	
	$r \times 10^3$	−0.22	−0.56	−0.65		$s \times 10^3$	−1.66	−0.89	−1.19	
	$t \times 10^3$	−0.52	−0.27	−0.32		$u \times 10^3$	+0.11	−0.04	+0.04	
NaF-K	$a \times 10^3$	+35.34	+69.49	+64.78	+74.40	$b \times 10^3$	+17.36	+21.81	+17.77	+19.50
	$c \times 10^3$	+2.53	+0.49	−2.18	−3.84	$d \times 10^3$	−9.13	+2.43	+2.43	+5.51
	$e \times 10^3$	+0.68	+4.18	+4.22	+4.61	$f \times 10^3$	+8.47	+9.72	+10.45	+10.67
	$g \times 10^3$	+2.24	+2.51	+2.36	+2.01	$h \times 10^3$	+3.73	+0.74	+1.26	+0.14
	$i \times 10^3$	+2.16	+3.93	+2.82	+2.68	$j \times 10^3$	−0.59	+0.72	−0.07	+0.03
	$k \times 10^3$	+0.81	+0.67	+0.34		$l \times 10^3$	+2.64	+0.65	+1.50	
	$m \times 10^3$	−0.91	+0.69	+0.54		$n \times 10^3$	−1.79	+0.94	+1.46	
	$p \times 10^3$	−0.17	+0.70	+0.72		$q \times 10^3$	+0.76	+0.06	+0.32	
	$r \times 10^3$	+0.02	+0.69	+0.73		$s \times 10^3$	+1.17	+1.17	+1.34	
	$t \times 10^3$	+0.33	+0.39	+0.37		$u \times 10^3$	−0.05	+0.03	−0.04	
KBr-Na	$a \times 10^3$	−20.77	−56.43	−47.75	−39.58	$b \times 10^3$	−6.12	−11.29	−8.28	−6.76
	$c \times 10^3$	+0.08	+0.01	+1.66	+1.30	$d \times 10^3$	−1.44	−12.39	−9.14	−5.95
	$e \times 10^3$	−1.49	−3.48	−3.09	−2.02	$f \times 10^3$	−2.88	−4.36	−4.18	−3.02
	$g \times 10^3$	−0.79	−0.45	−0.43	−0.24	$h \times 10^3$	−0.31	+0.75	+0.32	+0.09
	$i \times 10^3$	−0.91	−1.90	−1.38	−0.95	$j \times 10^3$	−0.16	−3.08	−2.29	−1.11
	$k \times 10^3$	−0.19	−0.06	+0.08		$l \times 10^3$	−0.26	+0.14	−0.18	
	$m \times 10^3$	−0.27	−1.44	−1.00		$n \times 10^3$	−0.55	−1.84	−1.26	
	$p \times 10^3$	−0.27	−0.27	−0.27		$q \times 10^3$	−0.09	+0.24	−0.02	
	$r \times 10^3$	−0.22	−0.52	−0.46		$s \times 10^3$	−0.36	−0.52	−0.56	
	$t \times 10^3$	−0.11	−0.01	−0.02		$u \times 10^3$	−0.01	−0.86	−0.56	

and fourth, eighth columns are calculations without ΔE_T by us and by Douglas, respectively. The small discrepancies of corresponding values will be due to the fact that we have considered the more displaced ions in the calculations than Douglas has shown in this table. In the first and fifth columns which are computations including the LST model, we note the next facts when they are compared with the columns "No ΔE_T."

(i) With respect to the movements of ions which are expressed with each parameter, in both cases of anion and cation impurities, *a*, *d*, *e*, *j*, *m*, *r*, and *u* have a tendency to decrease their absolute values, or to move in the opposite direction to the displacements of most ions in the crystals, compared with the corresponding parameters on the columns "No ΔE_T."

(ii) In both cases on anion and cation impurities, the parameters *h*, *k*, *l*, and *q* have a tendency to increase their absolute values, or to move in the oppo-

TABLE V. Lattice-relaxation parameters calculated by using each of two models of ΔE_T, and including covalency. In the calculation of these parameters such degree of covalency as shown in Table VI was used in order to get good agreements with the experimental EFG's. The types of covalency were also selected as written in the text.

Crystal		LST	RAA		LST	RAA		LST	RAA		LST	RAA
	$a\times10^3$	−16.24	−17.40	$b\times10^3$	+0.03	+0.06	$c\times10^3$	+0.18	+0.31	$d\times10^3$	−6.71	−6.92
	$e\times10^3$	+0.07	+0.02	$f\times10^3$	−0.13	−0.13	$g\times10^3$	+0.11	+0.13	$h\times10^3$	+0.02	+0.02
KBr-Cl	$i\times10^3$	−0.03	−0.03	$j\times10^3$	−3.18	−3.30	$k\times10^3$	+0.00	+0.01	$l\times10^3$	−0.01	−0.01
	$m\times10^3$	+0.04	+0.03	$n\times10^3$	−0.18	−0.15	$p\times10^3$	+0.05	+0.07	$q\times10^3$	+0.00	−0.00
	$r\times10^3$	−0.01	−0.01	$s\times10^3$	−0.04	−0.03	$t\times10^3$	+0.00	+0.00	$u\times10^3$	−1.25	−1.26
	$a\times10^3$	+115.15	+116.38	$b\times10^3$	+30.29	+25.17	$c\times10^3$	−0.53	−1.91	$d\times10^3$	+5.86	+15.63
	$e\times10^3$	+7.37	+7.28	$f\times10^3$	+17.49	+12.56	$g\times10^3$	+4.43	+2.23	$h\times10^3$	+2.92	−0.35
NaCl-K	$i\times10^3$	+4.71	+4.43	$j\times10^3$	−0.36	+2.98	$k\times10^3$	+1.17	+0.38	$l\times10^3$	+2.63	+0.57
	$m\times10^3$	+0.90	+2.08	$n\times10^3$	+3.26	+3.41	$p\times10^3$	+1.30	+0.97	$q\times10^3$	+0.72	−0.05
	$r\times10^3$	+1.20	+1.18	$s\times10^3$	+2.21	+1.50	$t\times10^3$	+0.71	+0.27	$u\times10^3$	−0.13	+0.54
	$a\times10^3$	−71.35	−77.72	$b\times10^3$	−6.91	−15.26	$c\times10^3$	−0.24	−0.92	$d\times10^3$	−15.26	−18.66
	$e\times10^3$	−4.20	−4.57	$f\times10^3$	−2.59	−6.51	$g\times10^3$	−0.45	−0.52	$h\times10^3$	+0.09	+1.37
KF-Na	$i\times10^3$	−1.16	−2.86	$j\times10^3$	−3.45	−3.53	$k\times10^3$	−0.07	−0.26	$l\times10^3$	−0.02	+0.34
	$m\times10^3$	−1.49	−2.11	$n\times10^3$	−1.34	−3.36	$p\times10^3$	−0.33	−0.40	$q\times10^3$	+0.01	+0.54
	$r\times10^3$	−0.46	−0.70	$s\times10^3$	−0.47	−0.70	$t\times10^3$	−0.04	−0.01	$u\times10^3$	−0.78	−0.96
	$a\times10^3$	+83.07	+93.56	$b\times10^3$	+16.22	+16.91	$c\times10^3$	+1.80	−0.14	$d\times10^3$	+8.86	+13.35
	$e\times10^3$	+5.27	+5.03	$f\times10^3$	+13.56	+9.66	$g\times10^3$	+3.18	+1.69	$h\times10^3$	+4.15	−0.19
NaF-K	$i\times10^3$	+2.10	+3.25	$j\times10^3$	−2.78	+1.53	$k\times10^3$	+1.05	+0.58	$l\times10^3$	+3.29	+0.49
	$m\times10^3$	−0.19	+1.47	$n\times10^3$	+4.41	+3.83	$p\times10^3$	+0.78	+0.74	$q\times10^3$	+0.81	−0.14
	$r\times10^3$	+0.85	+0.85	$s\times10^3$	+1.53	+1.13	$t\times10^3$	+0.63	+0.27	$u\times10^3$	−0.20	+0.06
	$a\times10^3$	−29.83	−56.43	$b\times10^3$	−6.02	−11.29	$c\times10^3$	+0.06	+0.01	$d\times10^3$	−4.52	−12.39
	$e\times10^3$	−2.05	−3.48	$f\times10^3$	−2.69	−4.36	$g\times10^3$	−0.68	−0.45	$h\times10^3$	−0.14	+0.75
KBr-Na	$i\times10^3$	−0.95	−1.90	$j\times10^3$	−0.77	−3.08	$k\times10^3$	−0.15	−0.06	$l\times10^3$	−0.13	+0.14
	$m\times10^3$	−0.56	−1.44	$n\times10^3$	−0.83	−1.84	$p\times10^3$	−0.30	−0.27	$q\times10^3$	−0.05	+0.24
	$r\times10^3$	−0.29	−0.52	$s\times10^3$	−0.37	−0.52	$t\times10^3$	−0.09	−0.01	$u\times10^3$	−0.13	−0.86

site direction to the displacements of most ions.

(iii) In the case of anion impurities, b, f, and s increase their absolute values except s in KBr-Cl.

These tendencies also are partially observed in the RAA model in the second and sixth columns. From these facts we recognize that participation of ΔE_T in the potential energy will increase the displacements of the ions due to impurity substitution toward (1,1,0) and (1,1,1) directions, and decrease those of the ions toward (1,0,0) direction. This effect of the three-body potentials resembles the failure of the Cauchy relations for the elastic constants in the pure ionic crystals discussed by Löwdin,[10,11] although there exists the difference that the former and latter are concerned with the inhomogeneous and homogeneous strains, respectively. These results are closely related to smallness of η at (1,1,0) sites in some crystals as shown later.

On the other hand, the values in Table V are generally much larger than the corresponding values in Table IV which suggests to us the serious effects of only several percent covalency upon the lattice relaxation accordingly upon the EFG. Of the lattice-relaxation parameters, $k, \ldots, u$ in Table V, several parameters are not so small compared with $a, \ldots, j$ that they can be neglected.

B. Electric field gradients

By using the lattice-relaxation parameters mentioned above and the electronic polarizations of Eq. (64), we have calculated the EFG, η and types of the EFG tensor on the various sites around impurity ions, according to the last section, and compared them with those of the experimental data in our paper RII or with the other worker's empirical results.[5,29–34] They are listed in Table VI where two kinds of calculated values are obtained independently by means of both models and where $eq = eq^i + eq^{el}$.

The Sternheimer antishielding factor, $1-\gamma_\infty$ and the constant k 's of the displaced ions in Eq. (67)

TABLE VI. Electric field gradients at various ion sites about impurity ions. EFG in units of 10^{12} esu/cm^3.

Crystal	Site	Model	Cov. (%)	Theoretical eq^i	eq^{el}	eq	Type	η	Experimental $\|eq\|$(Expt.)	Type	η
		LST	0	25.7	26.3	52.0[a]		0			
	Na(1,0,0)	RAA	0	22.1	29.9	52.0[a]		0	52		0
		LST	0	107.6	21.8	129.4	*B*	0.090			
NaCl-Br	Cl(1,1,0)	RAA	0	116.6	11.3	127.9	*B*	0.104	113	*B* or *C*	0.10
		LST	0	−7.8	0	−7.8		0			
	Na(1,1,1)	RAA	0	−6.1	0	−6.1		0	39		0
		LST	0	−19.5	−24.2	−43.7		0			
	Na(1,0,0)	RAA	0	−16.9	−26.6	−43.5		0	35		0
		LST	0	−125.4	−24.5	−149.9	*B*	0.086			
NaBr-Cl	Br(1,1,0)	RAA	0	−131.3	−14.8	−146.1	*B*	0.098	117	*B* or *C*	0.10
		LST	0	6.4	0	6.4		0			
	Na(1,1,1)	RAA	0	5.1	0	5.1		0	22		0
		LST	0	61.8	61.7	123.5		0			
	Na(1,0,0)	RAA	0	53.3	71.4	124.7		0	140		0
		LST	0	247.5	53.3	300.8	*B*	0.107			
NaCl-I	Cl(1,1,0)	RAA	0	275.4	28.0	303.4	*B*	0.098	339	*B* or *C*	0.10
		LST	0	−18.8	0	−18.8		0			
	Na(1,1,1)	RAA	0	−14.9	0	−14.9		0	91		0
		LST	0	−32.9	−51.1	−84.0		0			
	Na(1,0,0)	RAA	0	−29.0	−55.4	−84.4		0	54		0
NaI-Cl		LST	0	11.5	0	11.5		0			
	Na(1,1,1)	RAA	0	9.6	0	9.6		0	33		0
		LST	0	−21.0	−32.5	−53.5		0			
NaI-Br	Na(1,0,0)	RAA	0	−18.8	−35.8	−54.6		0	57		0
		LST	0	30.1	36.3	66.4		0			
	Na(1,0,0)	RAA	0	26.8	41.6	68.4		0	77		0
NaBr-I		LST	0	185.0	38.4	223.4	*B*	0.109			
	Br(1,1,0)	RAA	0	203.2	24.0	227.2	*B*	0.101	272.4	*B* or *C*	0.10
		LST	1.5	−97.3	0.13	−97.2	*A*	0.966			
KBr-Cl	Br(1,1,0)	RAA	0.9	−96.9	0.21	−96.7	*A*	0.920	99[b]	*A* or *D*	0.9
		LST	2.5	−789.2	368.5	−420.7		0			
	Cl(1,0,0)	RAA	3.0	−491.4	263.0	−228.4		0	421		0
		LST	2.5	60.1	36.3	96.4	*C*	0.099			
NaCl-K	Na(1,1,0)	RAA	3.0	61.8	34.0	95.8	*C*	0.032	97	*B* or *C*	0.10
		LST	2.5	121.8	0	121.8		0			
	Cl(1,1,1)	RAA	3.0	106.6	0	106.6		0	98		0
		LST	2.6	−136.6	−25.6	−162.2	*D*	0.644			
	K(1,1,0)	RAA	0.9	−141.9	−32.0	−173.9	*D*	0.411	180[c]	*A* or *D*	0.607
KF-Na		LST	2.6	−142.0	−112.9	−254.9		0			
	K(2,0,0)	RAA	0.9	−190.3	−78.4	−268.7		0	224.3[c]		0
		LST	0	−45.0	−27.7	−72.7	*C*	0.418			
	Na(1,1,0)	RAA	0	−52.1	−21.2	−73.3	*D*	0.125	75[d]	*A* or *D*	0.65
NaF-Li		LST	0	−126.9	19.5	−107.4		0			
	Na(2,0,0)	RAA	0	−100.0	−11.4	−111.4		0	118.3[d]		0

TABLE VI *(Continued).*

Crystal	Site	Model	Cov. (%)	Theoretical eq^{l}	eq^{el}	eq	Type	η	Experimental $\lvert eq\rvert$(Expt.)	Type	η
		LST	4.8	81.0	19.5	100.5	*D*	0.632			
	Na(1,1,0)	RAA	4.2	99.8	22.8	122.6	*D*	0.596	115[e]	*A* or *D*	0.45
NaF-K		LST	4.8	167.2	21.2	188.4		0			
	Na(2,0,0)	RAA	4.2	155.4	36.0	191.4		0	209.6[e]		0
		LST	0.9			−72.1		0.161			
KBr-Na	Br(2,1,0)	RAA	0			−137.1		0.213	75[b]		0.47

[a]In both models the calculated values of eq at the Na(1,0,0) site in this crystal were normalized to the empirical data in order to get "k" of the Na^+ ion.
[b]L. O. Andersson and E. Forslind, Refs. 30 and 31; W. D. Ohlsen and M. E. Melich, Ref. 32.
[c]A. Hartland, Ref. 33.
[d]K. F. Nelson and W. D. Ohlsen, Ref. 34; B. G. Dick and K. F. Nelson, Ref. 5.
[e]B.G. Dick and K. F. Nelson, Ref. 5. The other empirical data of EFG without alphabet have been obtained from our experiments as shown in the paper RII.

which were used in both models, are shown in Table VII. The $1-\gamma_\infty$ of the free ions were utilized for the Na^+ and K^+ ions because of small ions, while for the Cl^- and Br^- ions we have used the mean values of two evaluations each of which was determined by using the experimental $|eq|$'s and η's at (1,1,0)Cl or (1,1,0)Br sites in the crystals with anion impurities. The k's of Na^+ ion in both models were obtained from the eq^{el} at (1,0,0)Na in the NaCl-Br crystal so that the calculated eq on this site might be normalized to the experimental one. It will be noted that the $1-\gamma_\infty$ for large ions in the actual crystal is considerably smaller than that of the free ions.

In Table VI both models generally give the almost same evaluations and agree fairly well with the experimental EFG. The calculated eq's at (1,1,1) sites in various crystals are much smaller than the empirical ones [except (1,1,1)Cl in NaCl-K where agreement is quite good], the reason for which we cannot explain at present. For the (1,0,0), (1,1,0), and (2,0,0) sites the eq, η and types of the EFG tensor show comparatively good agreement with the experimental data. As stated in the introduction the measured η's on the (1,1,0) sites have the same values 0.10 for NaCl-Br, NaBr-Cl, NaCl-I, NaBr-I, and NaCl-K crystals. They are inconsistent with previous theory[2–5] which does not contain the ΔE_T. Good agreement of our calculated η by using both models with the measured one seems to originate in the fact that first, introducing E_T into the potential energy causes such a change of the displacements of ions as written in Sec. VII A, and secondly, the EFG calculation with eq^{el} also has a tendency to decrease the η in these crystals. The evaluated types of the EFG tensor in these crystals also agree with one of the empirically obtained types. The types *B* and *C* at (1,1,0) sites were found in this study for the first time, the latter of which is the type of (1,1,0)Na in NaCl-K crystal, and it will be discussed in the next section in connection with covalency.

TABLE VII. Sternheimer antishielding factor, $1-\gamma_\infty$ and deformation constants of electron shell, k used in two models.

Ion	Model	k (10^{15} esu/cm^3)	$1-\gamma_\infty$	$1-\gamma_\infty$ (Free ion)[a]
Na^+	LST	1.20	5.53	
	RAA	1.35	5.53	5.53
K^+	LST	3.70	13.8	
	RAA	2.10	13.8	13.8
Cl^-	LST	3.20	47.3	
	RAA	2.26	41.6	50.3
Br^-	LST	4.20	69.2	
	RAA	3.40	63.4	100

[a]Antishielding factors of free ions from T. P. Das and R. Bersohn, Phys. Rev. 102, 733 (1956); E. G. Wikner and T. P. Das, *ibid.* 109, 360 (1958).

The types and η's at (1,1,0)Na in NaF-Li crystal obtained by two models do not perfectly coincide with the experimental data although the eq's do very well with the empirical ones. Therefore we have tried to recalculate the EFG of this crystal, including a rotation effect of the off-center impurity Li^+ ion about the origin. But we could not obtain better results. It now seems that a quantum-mechanical treatment carried out by Quigley and Das[35] should be applied to this crystal.

We have calculated the EFG's in Table VI by using the TKS polarizabilities[23] as stated before. We have also computed them by means of the other three sets of polarizabilities, namely, TKS shell, Sternheimer and Sternheimer shell.[4] They are listed in Table VIII as an example in many computations. It will be obviously noted that the EFG's in these three schemes are nearly equal except Sternheimer's, consequently the different polarizabilities do not produce the large difference of the EFG in our calculation.

TABLE VIII. The eq and η calculated by using LST model in which only the polarizabilities of the ions were changed. The eq in units of 10^{12} esu/cm^3. The type of EFG tensors follows asymmetry-parameter values at the (1,1,0) sites. The 4th, 5th, 6th, and 7th columns represent the sets of TKS, TKS shell, Sternheimer and Sternheimer-shell polarizabilities, respectively (Refs. 4 and 6).

Crystal	Site		TKS	TKS-s	Steh	Steh-s
		eq	52.0	49.2	58.6	53.0
	(1,0,0)Na	η	0	0	0	0
NaCl-Br	(1,1,0)Cl	eq	129.4	133.7	117.0	127.6
		η	$0.090B$	$0.031B$	$0.250B$	$0.111B$
		eq	−7.8	−6.2	−11.2	−8.3
	(1,1,1)Na	η	0	0	0	0
		eq	123.5	116.8	139.1	125.7
	(1,0,0)Na	η	0	0	0	0
		eq	300.8	313.7	270.9	296.5
NaCl-I	(1,1,0)Cl	η	$0.107B$	$0.034B$	$0.280B$	$0.128B$
		eq	−18.8	−15.1	−26.5	−19.9
	(1,1,1)Na	η	0	0	0	0
		eq	−72.2	−68.8	−77.9	−73.1
	(1,1,0)Na	η	$0.418C$	$0.449C$	$0.525C$	$0.438C$
NaF-Li		eq	−107.3	−107.4	−118.1	−109.0
	(2,0,0)Na	η	0	0	0	0

C. Influence of covalent bonding on the EFG

Although it has not been expressed as a table, similar calculations to Sec. VII B were performed on the crystals with potassium ions, namely, KBr-Cl, NaCl-K, KF-Na, NaF-K, and KBr-Na. However, the computed EFG's do not agree with the experimental values.

As discussed in Sec. VI, due to the large overlap integrals between the nearest-neighbor ions, one of which is the potassium ion in these crystals, there will possibly exist a small quantity of covalent bonding between both ions which gives a great effect on the EFG. If we consider a small amount of covalency as shown in Table VI, agreements between calculations and experiments are satisfactory in both models where the types of covalency were taken as (iii), (ii), (i), (i), and (i) for KBr-Cl, NaCl-K, KF-Na, NaF-K, and KBr-Na crystals, with notation in Sec. VI, respectively (these types were selected in order to obtain good agreement). The dependences of eq, η and types of the EFG tensor on degree of covalency are described in Figs. 2–5 in which the solid lines show the results of computer calculation and the horizontal dotted lines express the empirical data, and the arrows represent the adequate degree of covalency to fit in with all the measured values.

For the (1,1,0)Br site in KBr-Cl, (1,1,0)Na and (1,1,1)Cl sites in NaCl-K, (1,1,0)K and (2,0,0)K sites in KF-Na, and (1,1,0)Na and (2,0,0)Na sites in NaF-K, both models give nearly equal EFG's and the same types of EFG, and they agree fairly well with the experimental values. Concerning the (1,0,0)Cl site in NaCl-K and the (2,1,0)Br site in KBr-Na, the RAA model does not show agreement with the empirical data, while the LST model does, as shown in Table VI. With respect to the (2,1,0)Br in KBr-Na, however, the calculated ϕ in Eq. (70) amounts to −25° 19′ for LST and to −28° 45′ for RAA; accordingly the direction cosines of the principal axes x', y', and z' relative to the x, y, and z crystal axes are $x'(0,0,1)$, $y'(0.904, -0.428, 0)$, and $z'(0.428, 0.904, 0)$ for LST, and $x'(0,0,1)$, $y'(0.877, -0.481, 0)$, and $z'(0.481, 0.877, 0)$ for RAA. They are nearly the same directions but do not agree with the measured values.[32]

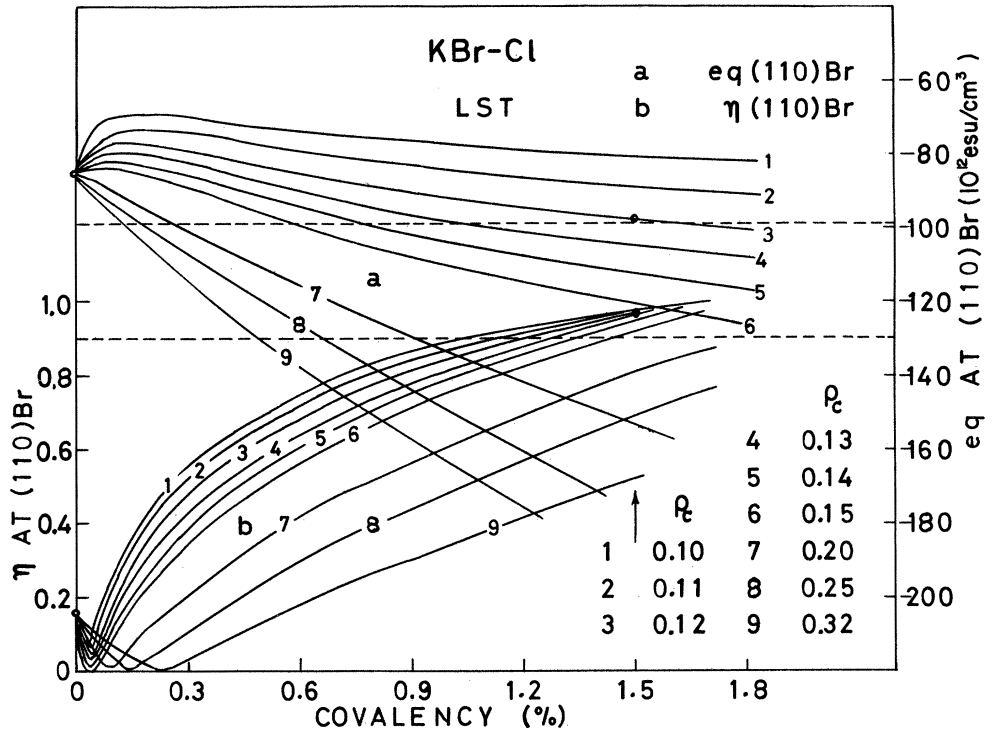

FIG. 2. The dependence of the EFG in KBr-Cl crystal obtained from LST model, on degree of covalency. The solid-line groups a and b represent eq at the (1,1,0)Br site and η at the same site calculated by using computer, respectively, and the horizontal dotted lines express the empirical data. The ρ_c denotes the denominator in the exponent of Eq. (75). Degree of covalency shown by an arrow gives the best agreement between theory and experiment.

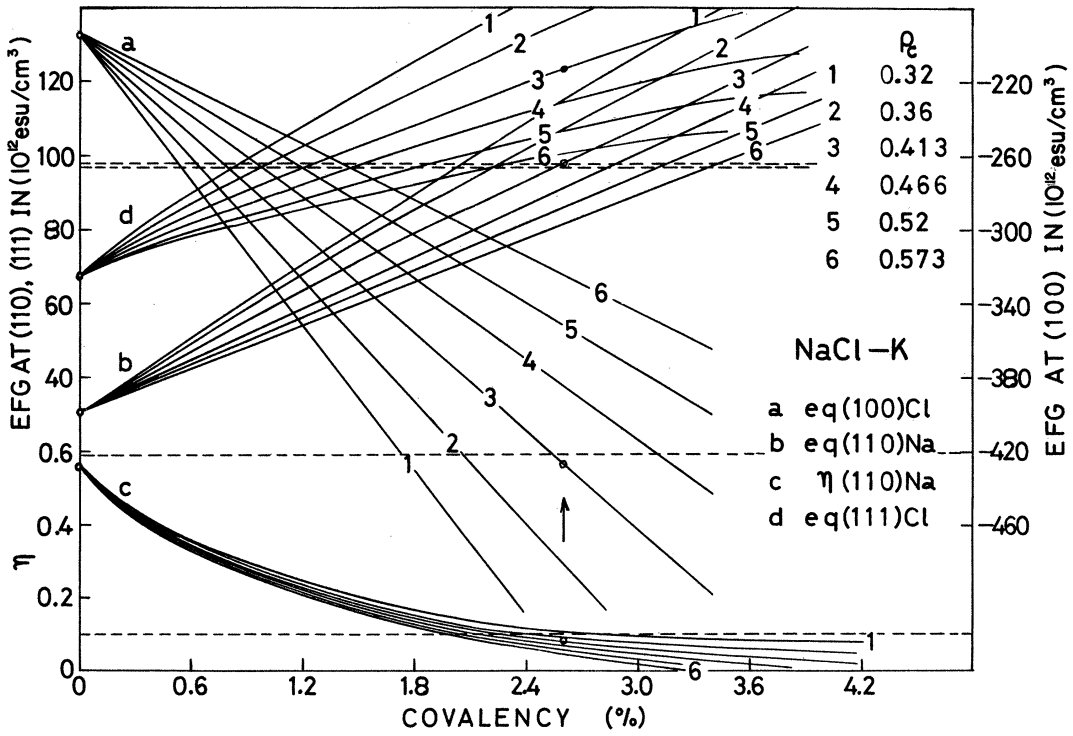

FIG. 3. The EFG at various sites in NaCl-K crystal calculated by using LST model, as a function of covalency. The dotted lines, ρ_c and an arrow express the things similar to those stated in Fig. 2.

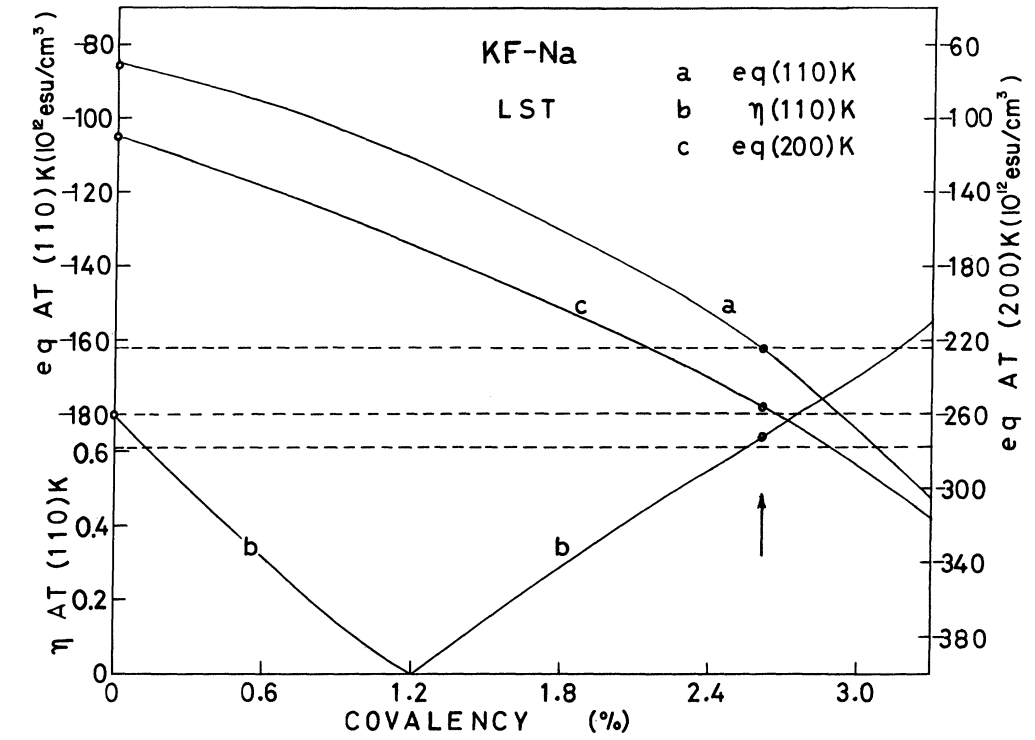

FIG. 4. The EFG in KF-Na crystal obtained from LST model vs degree of covalency. An arrow and the dotted lines represent the things similar to those stated in Fig. 2.

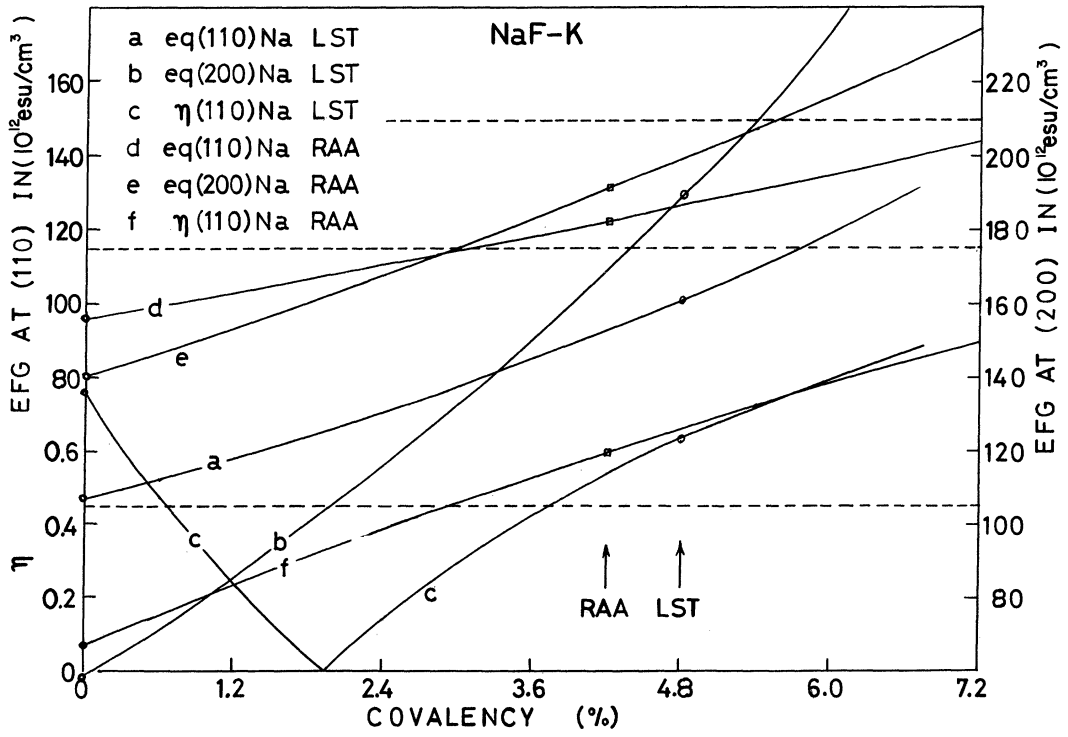

FIG. 5. The dependence of the EFG in NaF-K crystal calculated by using both models, on degree of covalency. The dotted lines and arrows express the things similar to those stated in Fig. 2.

D. Calculation including the nearest- and next-nearest-neighbor overlap integrals

So far we have discussed the effect of the overlaps and covalencies between the nearest-neighbor ions upon the lattice-relaxation parameters and the EFG (as for the overlap repulsion we took both nearest- and next-nearest-neighbor overlaps). As already stated in Secs. IV and V, we have also calculated these parameters and the EFG by taking ΔE_T with both the nearest- and second-neighbor overlap integrals in two models. In both models, however, the lattice-relaxation parameters evaluated in this way have shown the following special features: They are much smaller in "a," with about half value, while larger in the remaining parameters compared with those in the case in which nearest neighbors alone are considered, though the computational scheme certainly converges. Accordingly the eq 's which are derived from these parameters are much smaller than the empirical values (nearly half in some crystals), even if the adjustable parameters previously described are changed in their reasonable regions. Therefore it will be concluded that the second-neighbor anion pair overlap integrals in the actual crystals are negligibly small compared with the large second-neighbor ones of the AO's in the free ions.

VIII. SUMMARY AND CONCLUSION

We have calculated the electric field gradients, the asymmetry parameters η 's, and types of the EFG tensors on the sites similar to (1,0,0), (1,1,0), (1,1,1), (2,0,0), and (2,1,0) sites around the substitutional impurity ions in 12 ionic crystals including the three-body potentials by using Löwdin-Satoh-Taki or Ra-Abarenkov-Antonova models, and compared them with the values and types obtained from our experimental studies in RII[1] or from the other worker's empirical results. Generally in the crystals without K^+ ions, both models agree fairly well with the measured values, while for the crystals containing these ions agreement is achieved in both models by taking a small amount of covalency besides the large overlaps of the nearest-neighbor ions, one of which is the involved K^+ ion. With the LST model it is much easier to calculate the EFG's and results are considerably better in comparison with the experimental EFG's at (1,0,0)Cl in NaCl-K and at (2,1,0)Br in KBr-Na crystals than the RAA model as shown in Table VI.

The main features of this paper are inclusion of the three-center integrals within the potential energies and consideration of the electron-shell deformations originating in the displacements of the ions, and both are essential for calculations of the EFG since the conventional computations of the EFG without them cannot explain the experimental results. The new types of EFG tensors, B and C and also the small η 's have been found by us theoretically and experimentally for the first time. Our calculations about NaF-Li and KBr-Na crystals are not good enough and further investigations will be necessary.

By means of comparison between the computed and measured values of the EFG, it is inferred that the second-neighbor anion-pair overlap integrals in the actual ionic crystals are very small compared with the large ones in the free ions.

ACKNOWLEDGMENT

The authors would like to express their sincere thanks to Professor C. P. Slichter of University of Illinois for some valuable suggestions in this study.

[1] T. Taki and M. Satoh, Phys. Rev. B 23, 6721 (1981).
[2] B. G. Dick and T. P. Das, Phys. Rev. 127, 1053 (1962).
[3] T. P. Das and B. G. Dick, Phys. Rev. 127, 1063 (1962).
[4] B. G. Dick, Phys. Rev. 145, 609 (1966).
[5] B. G. Dick and K. F. Nelson, Phys. Rev. 186, 953 (1969).
[6] T. B. Douglas, J. Chem. Phys. 45, 4571 (1966).
[7] M. Satoh, K. Imaizumi, and T. Taki, J. Phys. Soc. Jpn. 38, 291 (1975).
[8] T. Taki and M. Satoh, Phys. Status Solidi B 71, K21 (1975).
[9] D. Ikenberry and T. P. Das, Phys. Rev. 184, 989 (1969).
[10] P. O. Löwdin, Ph.D. thesis (Almqvist and Wiksell, Uppsala, 1948) (unpublished).
[11] P. O. Löwdin, Adv. Phys. 5, 1 (1956).
[12] Ø. Ra, J. Chem. Phys. 52, 3765 (1970).
[13] I. V. Abarenkov and I. M. Antonova, Phys. Status Solidi B 38, 783 (1970).
[14] R. S. Mulliken, C. A. Rieke, D. Orloff, and H. Orloff, J. Chem. Phys. 17, 1248 (1949).
[15] D. W. Hafemeister and W. H. Flygare, J. Chem. Phys. 43, 795 (1965).
[16] M. Satoh and T. Taki, Phys. Rev. B 23, 6711 (1981).
[17] C. H. Townes and B. P. Dailey, J. Chem. Phys. 17, 782 (1949).
[18] N. F. Ramsey, Phys. Rev. 78, 699 (1950); 86, 243 (1952).
[19] A. Saika and C. P. Slichter, J. Chem. Phys. 22, 26 (1954).
[20] T. Kanda, J. Phys. Soc. Jpn. 10, 85 (1955).
[21] K. Yoshida and T. Moriya, J. Phys. Soc. Jpn. 11, 33 (1956).
[22] J. Kondo and J. Yamashita, J. Phys. Chem. Solids 10, 245 (1959).
[23] J. R. Tessman, A. H. Kahn, and W. Shockley, Phys. Rev. 92, 890 (1953).
[24] The e^2 and $e^2a_H^2$ are due to transformation from atomic to cgs units, and also $1/R_0$ and $1/R_0^3$ were considered for convenience of the calculation of potentials by computer so that the nearest-neighbor distance could be taken as one.

[25]M. P. Tosi, in *Solid State Physics,* edited by F. Seitz and D. Turnbull (Academic, New York, 1964), Vol. 16.
[26]Details of the computer programming will be published elsewhere in the future.
[27]The $C(2,0,0)$ and $D(1,1,1)$ sites designated by Das and Dick correspond to our D and C sites, respectively, as shown in Table I.
[28]T. P. Das and E. L. Hahn, in *Nuclear Quadrupole Resonance Spectroscopy, Solid State Physics Supplement 1,* edited by F. Seitz and D. Turnbull (Academic, New York, 1958).
[29]R. E. Slusher and E. L. Hahn, Phys. Rev. 166, 332 (1968).
[30]L. O. Andersson and E. Forslind, J. Chem. Phys. 38, 2303 (1963).
[31]L. O. Andersson and E. Forslind, Ark. Fys. 28, 49 (1964).
[32]W. D. Ohlsen and M. E. Melich, Phys. Rev. 144, 240 (1966).
[33]A. Hartland, Proc. R. Soc. London Ser. A 304, 361 (1968).
[34]K. F. Nelson and W. D. Ohlsen, Phys. Rev. 180, 366 (1969).
[35]R. J. Quigley and T. P. Das, Phys. Rev. 164, 1185 (1967).